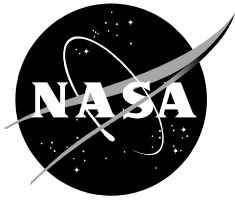


NASA Contractor Report NASA/CR-2006-214210



Forecasting Low-Level Convergence Bands Under Southeast Flow

William H. Bauman III
*Applied Meteorology Unit
Kennedy Space Center, Florida*

October 2006

NASA STI Program ... in Profile

Since its founding, NASA has been dedicated to the advancement of aeronautics and space science. The NASA scientific and technical information (STI) program plays a key part in helping NASA maintain this important role.

The NASA STI program operates under the auspices of the Agency Chief Information Officer. It collects, organizes, provides for archiving, and disseminates NASA's STI. The NASA STI program provides access to the NASA Aeronautics and Space Database and its public interface, the NASA Technical Report Server, thus providing one of the largest collections of aeronautical and space science STI in the world. Results are published in both non-NASA channels and by NASA in the NASA STI Report Series, which includes the following report types:

- **TECHNICAL PUBLICATION.** Reports of completed research or a major significant phase of research that present the results of NASA Programs and include extensive data or theoretical analysis. Includes compilations of significant scientific and technical data and information deemed to be of continuing reference value. NASA counterpart of peer-reviewed formal professional papers but has less stringent limitations on manuscript length and extent of graphic presentations.
- **TECHNICAL MEMORANDUM.** Scientific and technical findings that are preliminary or of specialized interest, e.g., quick release reports, working papers, and bibliographies that contain minimal annotation. Does not contain extensive analysis.
- **CONTRACTOR REPORT.** Scientific and technical findings by NASA-sponsored contractors and grantees.

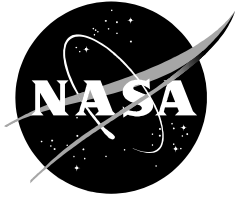
- **CONFERENCE PUBLICATION.** Collected papers from scientific and technical conferences, symposia, seminars, or other meetings sponsored or co-sponsored by NASA.
- **SPECIAL PUBLICATION.** Scientific, technical, or historical information from NASA programs, projects, and missions, often concerned with subjects having substantial public interest.
- **TECHNICAL TRANSLATION.** English-language translations of foreign scientific and technical material pertinent to NASA's mission.

Specialized services also include creating custom thesauri, building customized databases, and organizing and publishing research results.

For more information about the NASA STI program, see the following:

- Access the NASA STI program home page at <http://www.sti.nasa.gov>
- E-mail your question via the Internet to help@sti.nasa.gov
- Fax your question to the NASA STI Help Desk at (301) 621-0134
- Phone the NASA STI Help Desk at (301) 621-0390
- Write to:
NASA STI Help Desk
NASA Center for AeroSpace Information
7121 Standard Drive
Hanover, MD 21076-1320

NASA Contractor Report NASA/CR-2006-214210



Forecasting Low-Level Convergence Bands Under Southeast Flow

William H. Bauman III
*Applied Meteorology Unit
Kennedy Space Center, Florida*

October 2006

Acknowledgements

The author thanks Dr. Francis J. Merceret of the Kennedy Space Center Weather Office for his review and guidance and Ms. Katherine A. Winters of the 45th Weather Squadron for her feedback and suggestions.

Available from:

NASA Center for AeroSpace Information
7121 Standard Drive
Hanover, MD 21076-1320
(301) 621-0390

This report is also available in electronic form at

<http://science.ksc.nasa.gov/amu/>

Executive Summary

This report describes the work done by the Applied Meteorology Unit (AMU) in collecting and analyzing data from days with easterly flow in east-central Florida to try to determine what meteorological parameters affected the development, movement and dissipation of low-level convergence cloud bands over the Atlantic Ocean. During easterly flow events, the characteristics of the low-level convergence cloud bands influenced the meteorological conditions near Kennedy Space Center (KSC) and Cape Canaveral Air Force Station (CCAFS). On some days the cloud bands remained offshore and/or dissipated while on other days with seemingly similar synoptic conditions the cloud bands moved onshore and/or developed. The weather at KSC/CCAFS varied from clear skies to convective showers and thunderstorms depending on the cloud band behavior. The AMU compared and contrasted the atmospheric and thermodynamic conditions for all easterly flow events in the data set and found several discerning factors which determined the different weather phenomena occurring in the KSC/CCAFS vicinity.

The 45th Weather Squadron (45 WS) has stated that these widely varying conditions under what appears to be very similar weather regimes make it difficult to develop a forecast with high confidence. Of particular concern to the 45 WS were days with southeasterly synoptic flow when cloud bands were observed on satellite imagery in the Atlantic Ocean in the vicinity of The Bahamas. The forecasters have difficulty forecasting whether or not the clouds (which may contain precipitation and lightning) will make it to the KSC/CCAFS area. The forecasters have observed days when the cloud bands near The Bahamas dissipate prior to arrival at KSC/CCAFS and other days when they maintain their integrity and come onshore as low clouds or precipitation.

The AMU examined easterly flow events from April 2005 to February 2006. At the beginning of data collection portion of this task, the AMU discovered convergence cloud bands were present in many easterly flow situations, not just southeasterly flow as the 45 WS identified. During the analysis phase of this task, the AMU determined some of the easterly flow days were invalid because the dynamics were influenced by tropical cyclones or other synoptic scale features. Therefore, of the 33 easterly flow days collected and analyzed, 21 of those days were used to determine which parameters affected the behavior of the convergence cloud bands.

This report summarizes the composite meteorological conditions for the 21 event days with easterly flow. The general meteorological conditions were similar for days on which the cloud bands affected the KSC/CCAFS area and for days they did not. The AMU found subtle differences in the meteorological conditions that can explain the differences in cloud band behavior. The meteorological parameters that dictated the cloud band behavior and resultant weather conditions included the position of the low-level high pressure ridge, low-level wind speed and direction, location and movement of the east coast sea breeze front and upper level jet streak dynamics.

This report also presents two sample cases of easterly flow low-level convergence cloud band behavior. These cases depict one event in which the cloud bands developed and moved onshore and one event where the cloud bands dissipated over the open ocean.

Table of Contents

| | |
|--|----|
| Executive Summary..... | 3 |
| List of Tables..... | 8 |
| 1 Introduction..... | 9 |
| 1.1 Background and Objectives..... | 10 |
| 2 Methodology..... | 11 |
| 2.1 Identifying Easterly Flow Days..... | 11 |
| 2.2 Database of Potential Cases..... | 14 |
| 2.3 Data Set Summary..... | 14 |
| 3 Data Analysis..... | 16 |
| 3.1 Stability Analyses..... | 16 |
| 3.2 Sea Surface Temperature (SST)..... | 20 |
| 3.3 Low-level Phenomena..... | 23 |
| 3.4 Upper-level Phenomena..... | 24 |
| 3.5 Sea Breeze Effect..... | 26 |
| 4 Individual Case Studies..... | 28 |
| 4.1 Convergence Cloud Band Day – 20 July 2005..... | 28 |
| 4.1.1 Analysis of Low-level Features..... | 29 |
| 4.1.2 Analysis of Upper-level Features..... | 30 |
| 4.2 No Convergence Cloud Band Formation – 16 May 2005..... | 31 |
| 4.2.1 Analysis of Low-level Features..... | 32 |
| 4.2.2 Analysis of Upper-level Features..... | 34 |
| 5 Summary and Conclusions..... | 36 |
| 5.1 Important Forecast Indicators..... | 36 |
| 5.1.1 East-central Florida Low-Level Parameters..... | 36 |
| 5.1.2 East-central Florida Upper-Level Parameters..... | 36 |
| 5.2 Combining the Low- and Upper-Level Indicators..... | 37 |
| References..... | 38 |

List of Figures

| | | |
|------------|--|----|
| Figure 1. | Satellite image on 5 February 2004 at 1824 UTC from the NOAA-16 polar-orbiting environmental satellite Advanced Very High Resolution Radiometer (AVHRR) sensor. A convergence cloud band is visible extending from just north of The Bahamas to the KSC/CCAFS area during conditions with a southeasterly synoptic wind flow regime..... | 9 |
| Figure 2. | Visible satellite image on 7 July 2005 at 1845 UTC from the GOES East satellite. Convergence cloud bands can be seen developing downwind of islands in The Bahamas. | 11 |
| Figure 3. | Example of the RUC analysis mean 1000-700 mb wind speed and direction used to identify easterly flow days..... | 12 |
| Figure 4. | Example of the ARPS analysis 10 m (surface) wind speed and direction and mean sea level pressure used to identify easterly flow days..... | 12 |
| Figure 5. | Map showing the locations of the four RAOB sites (red text) used to help identify easterly flow days: Nassau (MYNN), Miami (MFL), Cape Canaveral (XMR) and Jacksonville (JAX). | 13 |
| Figure 6. | Map showing the locations of the surface observation sites used to help identify easterly flow days. The locations in red are land-based METAR stations and the locations in blue are fixed buoys. | 13 |
| Figure 7. | The average height (mb) of the inversion in morning soundings at MYNN, MFL and XMR from the days shown in Table 1. The light blue columns represent days when cloud bands reached the shore and the green columns represent days when the cloud bands were not present or did not reach the shore..... | 16 |
| Figure 8. | The average height (mb) of the inversion from morning soundings at XMR. If there was no inversion, the text “NO Inv” is displayed. The light blue columns represent days when cloud bands reached the shore and the green columns represent days when the cloud bands were not present or did not reach the shore. | 17 |
| Figure 9. | The average Lifted Index from morning soundings at MYNN, MFL and XMR. The light blue columns represent days when cloud bands reached the shore and the green columns represent days when the cloud bands were not present or did not reach the shore. The solid black line is the second order polynomial trend line. | 17 |
| Figure 10. | The average K Index from morning soundings at MYNN, MFL and XMR. The light blue columns represent days when cloud bands reached the shore and the green columns represent days when the cloud bands were not present or did not reach the shore. The solid black line is the second order polynomial trend line. | 18 |
| Figure 11. | The average SWEAT from morning soundings at MYNN, MFL and XMR. The light blue columns represent days when cloud bands reached the shore and the green columns represent days when the cloud bands were not present or did not reach the shore. The solid black line is the second order polynomial trend line. | 18 |
| Figure 12. | The average Total Totals from morning soundings at MYNN, MFL and XMR. The light blue columns represent days when cloud bands reached the shore and the green columns represent days when the cloud bands were not present or did not reach the shore. The solid black line is the second order polynomial trend line. | 19 |
| Figure 13. | The average CAPE from morning soundings at MYNN, MFL and XMR. The light blue columns represent days when cloud bands reached the shore and the green columns represent days when the cloud bands were not present or did not reach the shore. The solid black line is the second order polynomial trend line. | 19 |
| Figure 14. | Example of the SST single pass image from the Rutgers University Marine and Coastal Sciences web site on 19 May 2006 at 2128 UTC from the NOAA-12 satellite..... | 20 |
| Figure 15. | Example of a SST 3-day composite image from the USF Institute for Remote Sensing web site. The three solid black circles indicate the locations used in this study to retrieve SST for analysis. The date over the USF symbol is the middle of the three days 18-20 May 2006..... | 21 |

| | |
|---|----|
| Figure 16. The SST values just offshore XMR on all the case study days. The light blue columns represent days when cloud bands reached the shore and the green columns represent days when the cloud bands were not present or did not reach the shore. | 21 |
| Figure 17. The SST differences on all the case study days between the region just offshore XMR and MYGW (see Figure 15). The light blue columns represent days when cloud bands reached the shore and the green columns represent days when the cloud bands were not present or did not reach the shore. | 22 |
| Figure 18. The maximum SST between XMR and MYGW (see Figure 15) on all the case study days. The light blue columns represent days when cloud bands reached the shore and the green columns represent days when the cloud bands were not present or did not reach the shore. | 22 |
| Figure 19. The average wind speed in the layer from surface to 700 mb from XMR. The light blue columns represent days when cloud bands reached the Florida shore and the green columns represent days when the cloud bands were not present or did not reach the shore. | 23 |
| Figure 20. The RUC 6-hour layer average 1000 mb – 700 mb wind forecast valid 21 UTC superimposed on the visible satellite image on 16 August 2005 at 1815 UTC from the GOES East satellite. The yellow arrow represents the wind flow around the low-level high pressure area. The low-level high pressure ridge position is shown by the solid blue jagged line. | 24 |
| Figure 21. The Uccellini four quadrant straight jet streak model showing the ageostrophic horizontal and vertical motions (Uccellini and Kocin 1987). | 25 |
| Figure 22. Visible satellite image on 20 May 2005 at 1745 UTC with (a) 250 mb wind barbs and isotachs (isotachs are shaded at 50, 60, 70, 80 and 90 knots) from the Eta 6 hour forecast valid at 1800 UTC overlaid and (b) the center line of the 250 mb jet and the jet left and right entrance regions from (a) depicted for clarity. | 25 |
| Figure 23. Visible satellite images on 16 August 2005 at (a) 1315 UTC with surface observations and low-level streamlines overlaid, (b) 1445 UTC with surface observations and low-level streamlines overlaid, (c) 1631 UTC with surface observations, low-level streamlines overlaid and the position of the sea breeze front overlaid and (d) 1815 UTC with surface observations, low-level streamlines and the position of the sea breeze front overlaid. | 27 |
| Figure 24. Visible satellite image on 20 July 2005 at 1540 UTC from the GOES East satellite. The Eta surface wind and streamline analysis at 1200 UTC is overlaid on the satellite image. The wind barbs are plotted in yellow and speed is in knots. The streamlines are depicted by the solid orange lines. The low-level high pressure ridge position is shown by the solid blue line near JAX. | 28 |
| Figure 25. The 0.5° reflectivity image from the NWS MLB WSR-88D radar on 20 July 2005 at 1854 UTC. Precipitating cloud bands can be seen southeast of KSC/CCAFS with reflectivity values up to 45 dBZ. | 29 |
| Figure 26. Eta 6-hour surface wind and streamline forecast valid 20 July 2005 at 1800 UTC as in Figure 24. The Eta data is superimposed on the visible satellite image on 20 July 2005 at 1815 UTC. | 30 |
| Figure 27. Eta 6-hour 250 mb wind forecast valid 20 July 2005 at 1800 UTC. Wind barbs are in green and knots. Isotachs are shaded at 30, 40 and 50 knots. The Eta data is superimposed on the visible satellite image on 20 July 2005 at 1815 UTC. The position of the east coast sea breeze front is shown in cyan. | 31 |
| Figure 28. Visible satellite image on 16 May 2005 at 1745 UTC from the GOES East satellite. The Eta 6-hour forecast surface streamline analysis at 1800 UTC is overlaid on the satellite image as the green solid lines with arrows. The low-level high pressure ridge position is shown by the solid blue line. The position of the east coast sea breeze front is shown in cyan. Convergence cloud bands can be seen in the Atlantic Ocean east of southeast Florida and extending northwest from Grand Bahama Island. | 32 |
| Figure 29. MFL sounding on 16 May 2005 at 1200 UTC. Vertical wind profile from surface to 700 mb is shown inside the red ellipse. | 33 |
| Figure 30. XMR sounding on 16 May 2005 at 1000 UTC. Vertical wind profile from surface to 700 mb is shown inside the red ellipse. | 33 |

- Figure 31. JAX sounding on 16 May 2005 at 1200 UTC. Vertical wind profile from surface to 700 mb is shown inside the red ellipse.34
- Figure 32. Eta 6-hour 250 mb wind forecast valid 16 May 2005 at 1800 UTC. Wind barbs (knots) are in green. Isotachs are shaded at 50, 60, 70, 80 and 90 knots. The Eta data is superimposed on the visible satellite image on 16 May 2005 at 1745 UTC. The position of the east coast sea breeze front is shown in cyan...35

List of Tables

Table 1. Summary of easterly flow dates for which data was collected.....15

1 Introduction

Easterly synoptic flow can bring a wide variety of weather to the Kennedy Space Center (KSC) and Cape Canaveral Air Force Station (CCAFS) area – from clear skies to convective showers and thunderstorms. Clouds and precipitation affect a multitude of operations from daily ground processing to space launches and landings. The 45th Weather Squadron (45 WS) has stated that these widely varying conditions under what appears to be very similar weather regimes make it difficult to develop a forecast with high confidence. Of particular concern to the 45 WS are days with southeasterly synoptic flow when cloud bands are observed on satellite imagery in the Atlantic Ocean in the vicinity of The Bahamas. The forecasters have difficulty forecasting whether or not the cloud bands, which may contain precipitation and lightning, will make it to the KSC/CCAFS area. The forecasters have observed days when the cloud bands near The Bahamas dissipate prior to arrival at KSC/CCAFS and other days when they maintain their integrity and come onshore as low clouds or precipitation. Figure 1 shows a satellite image on 5 February 2004 at 1824 UTC from the NOAA-16 polar-orbiting environmental satellite Advanced Very High Resolution Radiometer (AVHRR) sensor. A convergence cloud band is visible extending from just north of The Bahamas to the KSC/CCAFS area during conditions with a southeasterly synoptic wind flow regime.

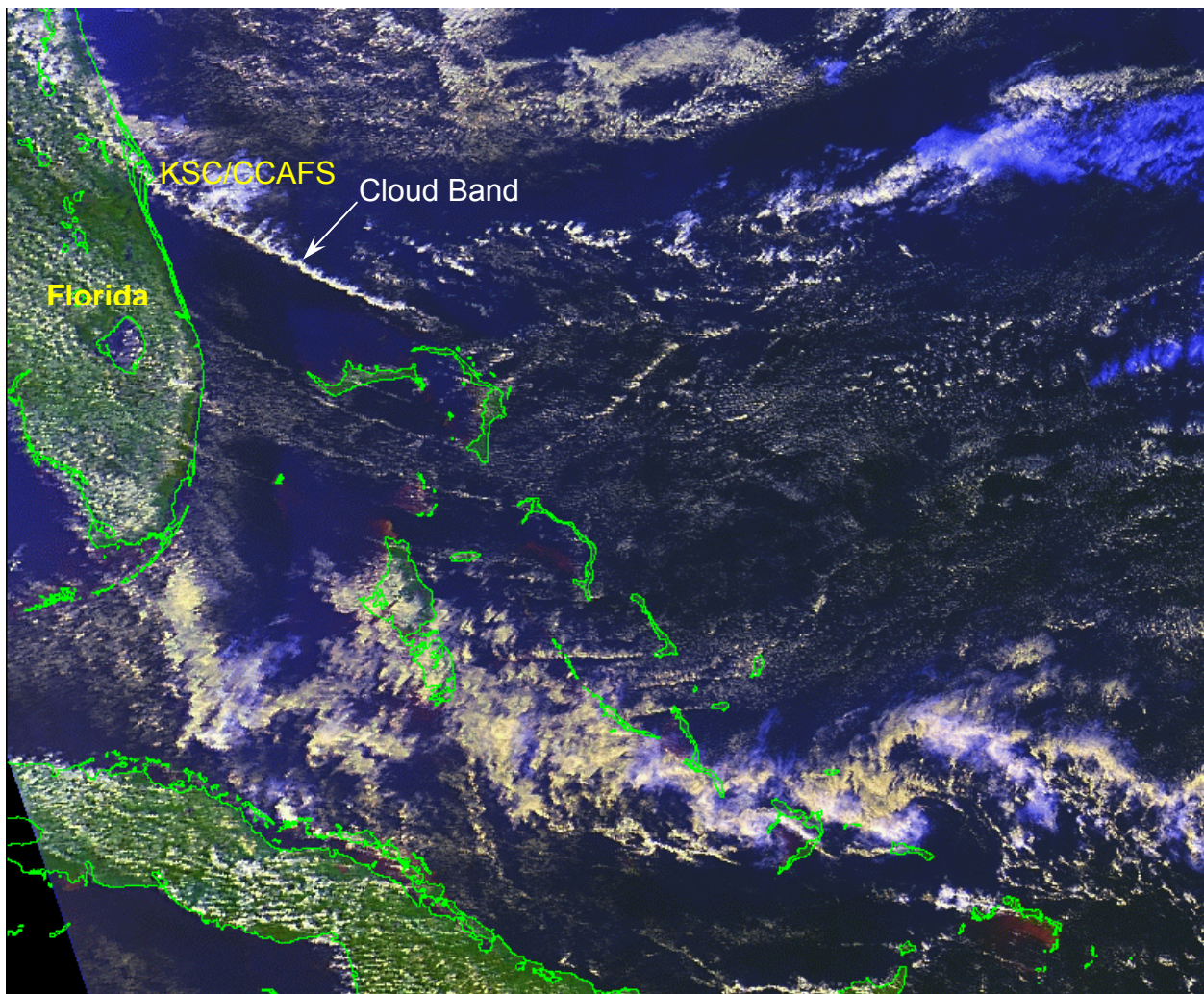


Figure 1. Satellite image on 5 February 2004 at 1824 UTC from the NOAA-16 polar-orbiting environmental satellite Advanced Very High Resolution Radiometer (AVHRR) sensor. A convergence cloud band is visible extending from just north of The Bahamas to the KSC/CCAFS area during conditions with a southeasterly synoptic wind flow regime.

1.1 Background and Objectives

As described in the introduction, convergence cloud bands forming under southeasterly synoptic flow can lead to missed cloud, rain, and thunderstorm forecasts. They occur any time of year and are a difficult forecast problem. Therefore, the 45 WS requested that the Applied Meteorology Unit (AMU) try to provide forecast guidance on when these convergence bands occur and do not occur. During the data acquisition portion of this task, the AMU discovered that the convergence cloud band phenomenon not only occurred during southeasterly synoptic flow but during all synoptic flow conditions with an easterly component. Therefore, the AMU analyzed days when any synoptic onshore flow occurred.

The AMU decided to acquire the data in real time because preliminary analysis during the proposal response phase of the task indicated the development and maintenance of convergence bands appeared to be controlled by mesoscale phenomena/dynamics – in the boundary layer and/or at upper levels. Therefore, this task required use of a high resolution mesoscale model to look for subtle differences in the mesoscale dynamics that appeared to be driving the cloud band development. Since such high resolution model data was not readily available in an existing archive, the AMU archived data from synoptic easterly flow events in real-time to build a database of cases for analysis. These “events” included days when no convergence bands developed, days when convergence bands developed but did not maintain themselves and did not affect KSC/CCAFS, days when convergence bands developed and maintained their integrity all the way to KSC/CCAFS resulting in local convection. The AMU ran the Advanced Regional Prediction System (ARPS) model on the AMU numerical weather prediction (NWP) modeling cluster at least 4 times per day and archived the high resolution model output as part of the database.

A literature review revealed very little recent research has been conducted on this subject. The most significant amount of recent work has been done in Hawaii. The Atlantic Trade Wind Experiment (ATEX) was conducted in 1969 and is described in papers by the original participants (e.g., Augstein et al. 1973, 1974; Brümmer et al. 1974).

The main objectives of this task included:

- Formulating a database of days with easterly synoptic flow using real time data acquisition,
- Analyzing and identify parameters thought to contribute to formation of convergence cloud bands,
- Documenting the conditions favorable and unfavorable to convergence band development, and
- Delivering a final report, a forecaster tool or nomogram.

2 Methodology

The 45 WS forecasters and Launch Weather Officers (LWOs) indicated the easterly flow events take place anytime of year but are prevalent in the warm season from May through September. The convergence cloud bands over the open ocean are most easily detected with Geostationary Operational Environmental Satellites (GOES) visible satellite imagery and frequently are observed forming in the lee of the Islands of The Bahamas during the daytime as shown in Figure 2. The cloud bands are much more difficult to detect with infrared imagery since they are low, warm clouds while developing.

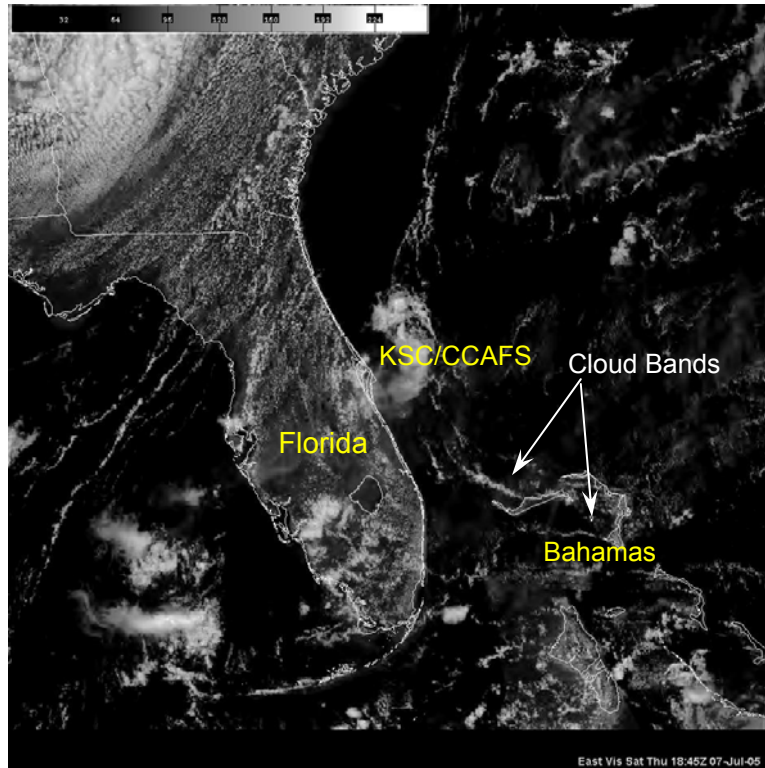


Figure 2. Visible satellite image on 7 July 2005 at 1845 UTC from the GOES East satellite. Convergence cloud bands can be seen developing downwind of islands in The Bahamas.

Since there were few documented cases archived, the AMU collected data in near real-time beginning in April 2005 and ending in March 2006 on days when easterly flow was present at KSC/CCAFS. Data was collected and saved for analysis using the ENSCO, Inc. MetWise™ Net meteorological PC workstation. MetWise Net is a commercial version of the National Oceanic and Atmospheric Administration (NOAA) Earth System Research Laboratory (ESRL) Global Systems Division (GSD) FX-Net. MetWise Net provides access to the basic display capability of an Advanced Weather Interactive Processing System (AWIPS) workstation via the Internet. MetWise Net emulates the AWIPS workstation graphical user interface very closely.

2.1 Identifying Easterly Flow Days

The AMU identified easterly flow days by using the mean 1000-700 mb wind direction and/or mean surface wind direction from the Rapid Update Cycle (RUC) analysis (Figure 3), Advanced Regional Prediction System (ARPS) surface winds analysis (Figure 4), radiosonde observations (RAOB) and surface observations. Surface winds were used to determine easterly flow days primarily on days when the mean 1000-700 mb layer contained directional shear resulting in a nearly calm mean wind in the layer with non-representative directionality. The RAOBs used were from Nassau (MYNN), Miami (MFL), Cape Canaveral (XMR) and Jacksonville (JAX) as shown in Figure 5. The surface observations used included all those available from The Bahamas, the eastern half of peninsular Florida, stationary buoys and moving maritime (Figure 6).

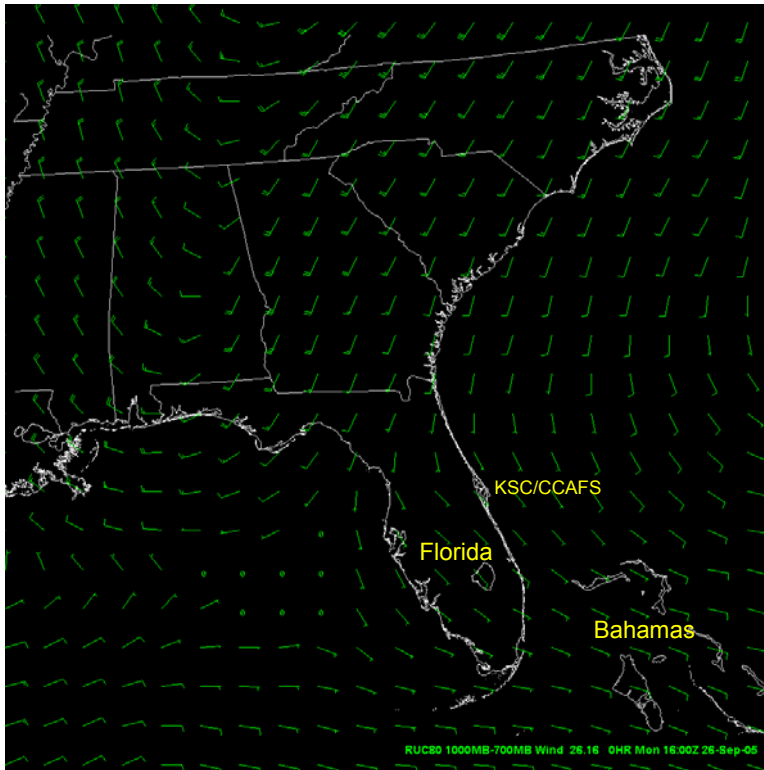


Figure 3. Example of the RUC analysis mean 1000-700 mb wind speed and direction used to identify easterly flow days.

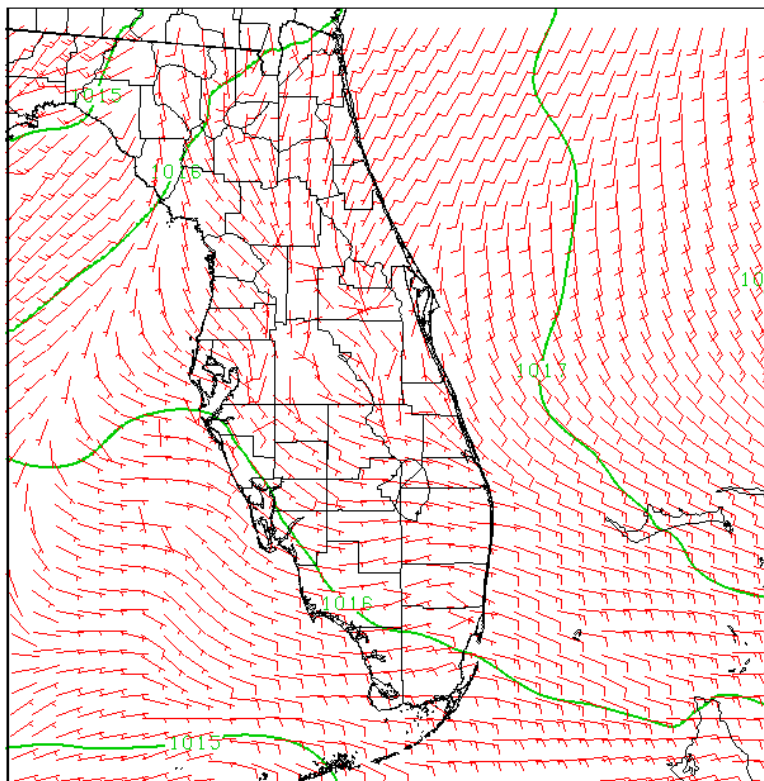


Figure 4. Example of the ARPS analysis 10 m (surface) wind speed and direction and mean sea level pressure used to identify easterly flow days.

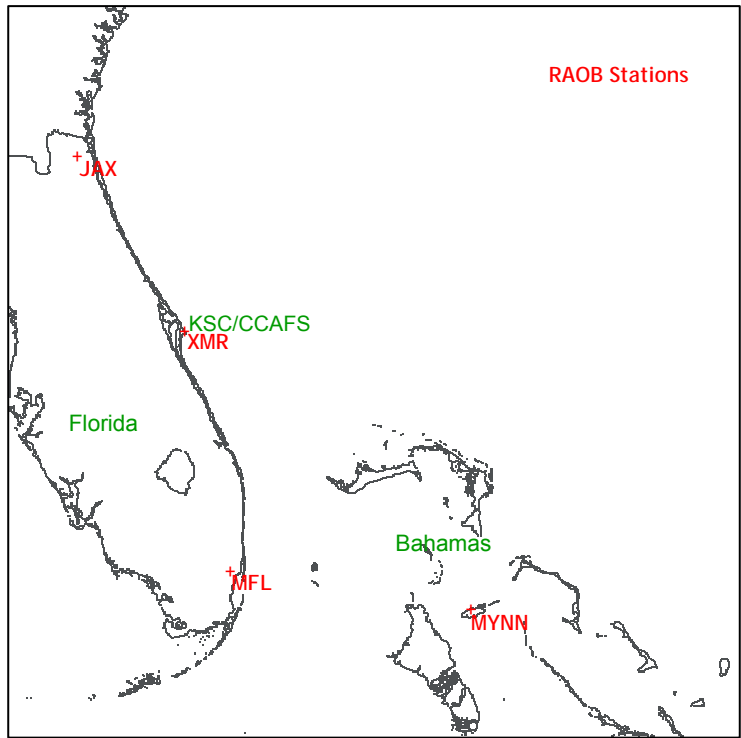


Figure 5. Map showing the locations of the four RAOB sites (red text) used to help identify easterly flow days: Nassau (MYNN), Miami (MFL), Cape Canaveral (XMR) and Jacksonville (JAX).

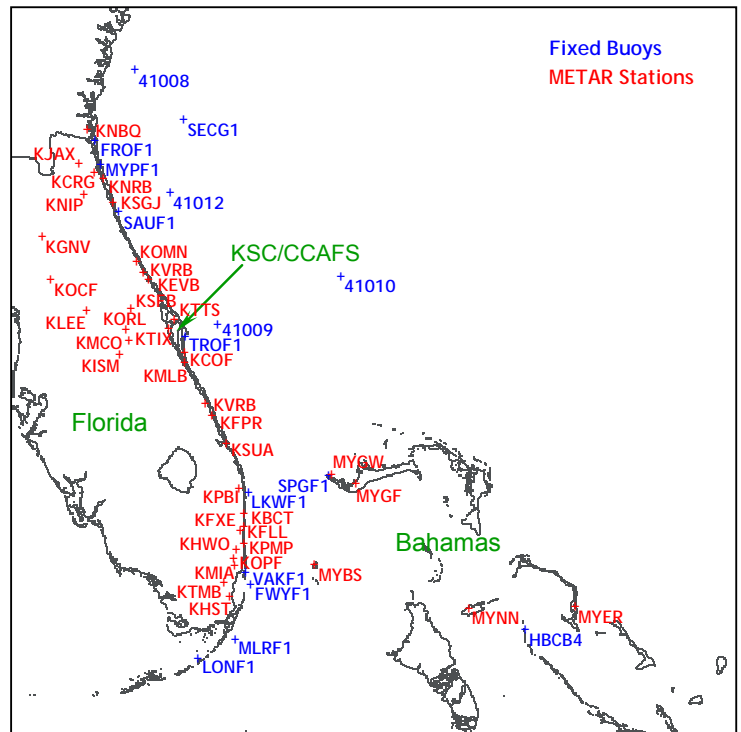


Figure 6. Map showing the locations of the surface observation sites used to help identify easterly flow days. The locations in red are land-based METAR stations and the locations in blue are fixed buoys.

2.2 Database of Potential Cases

Several theories regarding the most likely meteorological criteria and dynamics causing the convergence cloud bands to form were proposed by AMU staff and AMU customers at the onset of this task. Based on the literature review and discussions with 45 WS personnel and forecasters at the National Weather Service Forecast Office in Melbourne (NWS MLB), the AMU collected the following parameters for analysis:

- Low-level high pressure ridge position,
- Upper-level jet streak or speed max position,
- Surface wind speed,
- Surface wind direction,
- Average wind speed and direction ≤ 700 mb,
- Average wind speed and direction ≥ 500 mb,
- Maximum height of the easterly winds,
- Sea surface temperature (SST) difference between Cape Canaveral and West End, Grand Bahama,
- Average height of the inversion base, inversion top, CCL, LFC, and LCL from the soundings at MYNN, MFL and XMR,
- Temperatures from XMR at 500 mb, 400 mb, 300 mb, 250 mb, 200 mb, 150 mb, and 100 mb, and
- Temperature difference across peninsular Florida at 500 mb, 400 mb, 300 mb, 250 mb, 200 mb, 150 mb, and 100 mb.
- Stability parameters.

The following additional observational data were collected to verify presence or lack of convergence cloud bands, precipitation and lightning:

- Radar data from the Melbourne and Miami Weather Surveillance Radar-1988 Doppler (WSR-88D) to include:
 - 0.5° elevation angle radar reflectivity,
 - Composite reflectivity and
 - 0.5° elevation angle radar velocity.
- Visible satellite imagery,
- Infrared satellite imagery,
- Water vapor satellite imagery and
- Lightning data from the National Lightning Detection Network (NLDN).

After identifying potential cases, the AMU examined visible satellite imagery to confirm whether the day had convergence cloud band development, existing convergence cloud bands or no cloud bands and whether or not the cloud bands moved onshore or remained over open water. If cloud bands were observed in the visible satellite imagery, the radar reflectivity data was examined to determine if precipitation was present and if the precipitation made it onshore or remained over open water. Finally, if precipitation was observed, lightning data was examined to determine if cloud-to-ground lightning was detected. These three data sources were entered into an Excel spreadsheet prior to analysis of all the data collected.

2.3 Data Set Summary

From April 2005 through February 2006, the AMU collected and analyzed data from 33 days with easterly flow (Table 1). The initial analysis indicated some of the cases collected were not “typical” easterly flow days. Easterly flow was present on these atypical days but the weather in the KSC/CCAFS area was influenced by other phenomena such as upper level cut off lows, tropical cyclones, and synoptic fronts. The days on which these phenomena occurred were not used in the data analysis and are shown in red text in Table 1.

Table 1. Summary of easterly flow events for which data was collected.
 The numbers in each column correspond to the day of the month when the event occurred.

| 2005 | | | | | | | | | 2006 | |
|------|-----|-----|-----|-----|-----|-----|-----|-----|------|-----|
| Apr | May | Jun | Jul | Aug | Sep | Oct | Nov | Dec | Jan | Feb |
| 5 | 12 | 9 | 7 | 15 | 19 | 3 | 4 | 14 | 20 | 16 |
| 11 | 13 | 14 | 20 | 16 | 26 | 11 | 14 | | | |
| 12 | 16 | 27 | 25 | 18 | 28 | | 15 | | | |
| | 17 | 28 | | 23 | | | | | | |
| | 18 | | | 24 | | | | | | |
| | 19 | | | | | | | | | |
| | 20 | | | | | | | | | |

3 Data Analysis

This section summarizes the analysis of the various data types collected for this task.

3.1 Stability Analyses

Chen and Feng (2001) indicated inversion base height, inversion depth and other stability parameters could play a role in cloud band development, maintenance and decay. One observation they made was that on days with a higher inversion height, more net diabatic heating was released as clouds developed resulting in stronger upward vertical motion. Figure 7 shows the average height of the inversion base from the morning soundings at MYNN, MFL and XMR from the days in Table 1. Unfortunately, the data does not support the observations from Chen and Feng. The average height of the inversion base only varied by 10 mb between days with and days without cloud bands, and was lower on days with cloud bands. The height of the inversion base at XMR was also calculated for each day from the 1000 UTC sounding (Figure 8). Similar to the average for all three sounding sites, there was little difference in the height of the inversion base on days with cloud bands and days without cloud bands. The average difference for XMR was only 8 mb, but was higher on days with cloud bands.

Other stability parameter were calculated from the soundings and analyzed, including Lifted Index, K Index, Severe Weather Threat Index (SWEAT), Total Totals and Convective Available Potential Energy (CAPE). In every one of these parameters, the only apparent signal found was seasonal, as shown in Figure 9 (Lifted Index), Figure 10 (K Index), Figure 11 (SWEAT), Figure 12 (Total Totals) and Figure 13 (CAPE). Based on this data set, the AMU could not uncover any stability parameters from the sounding sites in Florida or The Bahamas that were directly related to the development or maintenance of cloud bands.

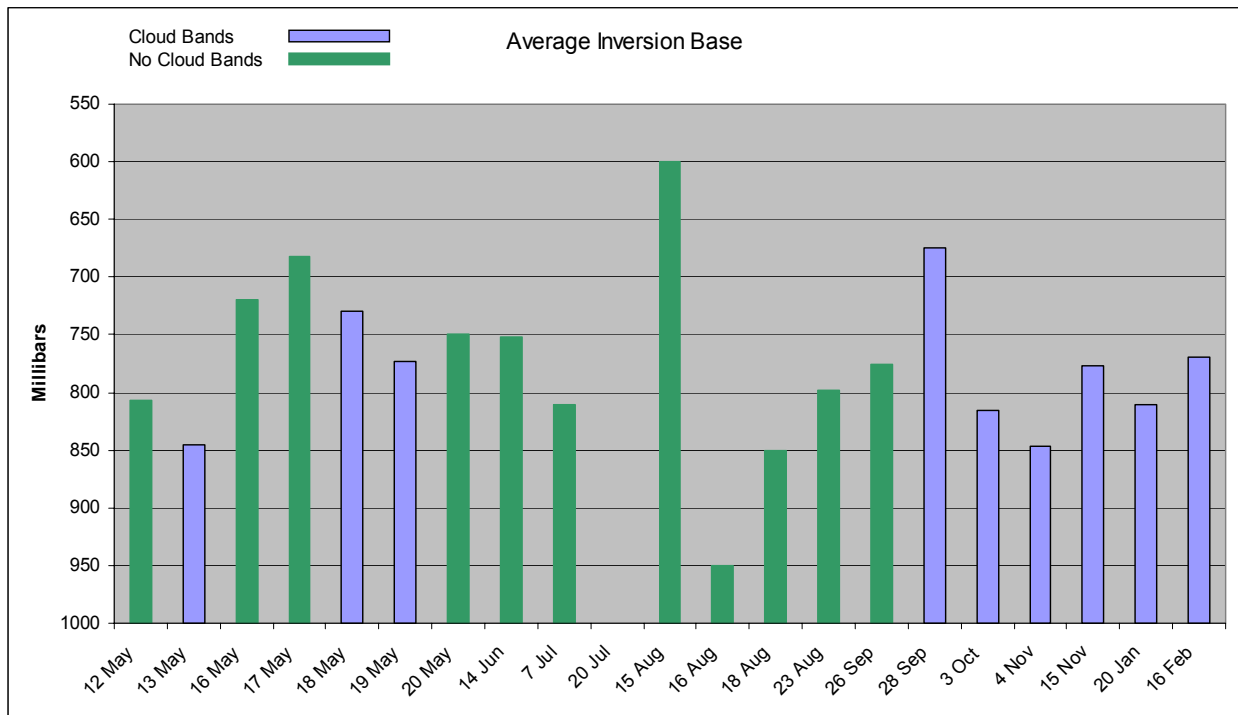


Figure 7. The average height (mb) of the inversion in morning soundings at MYNN, MFL and XMR from the days shown in Table 1. The light blue columns represent days when cloud bands reached the shore and the green columns represent days when the cloud bands were not present or did not reach the shore.

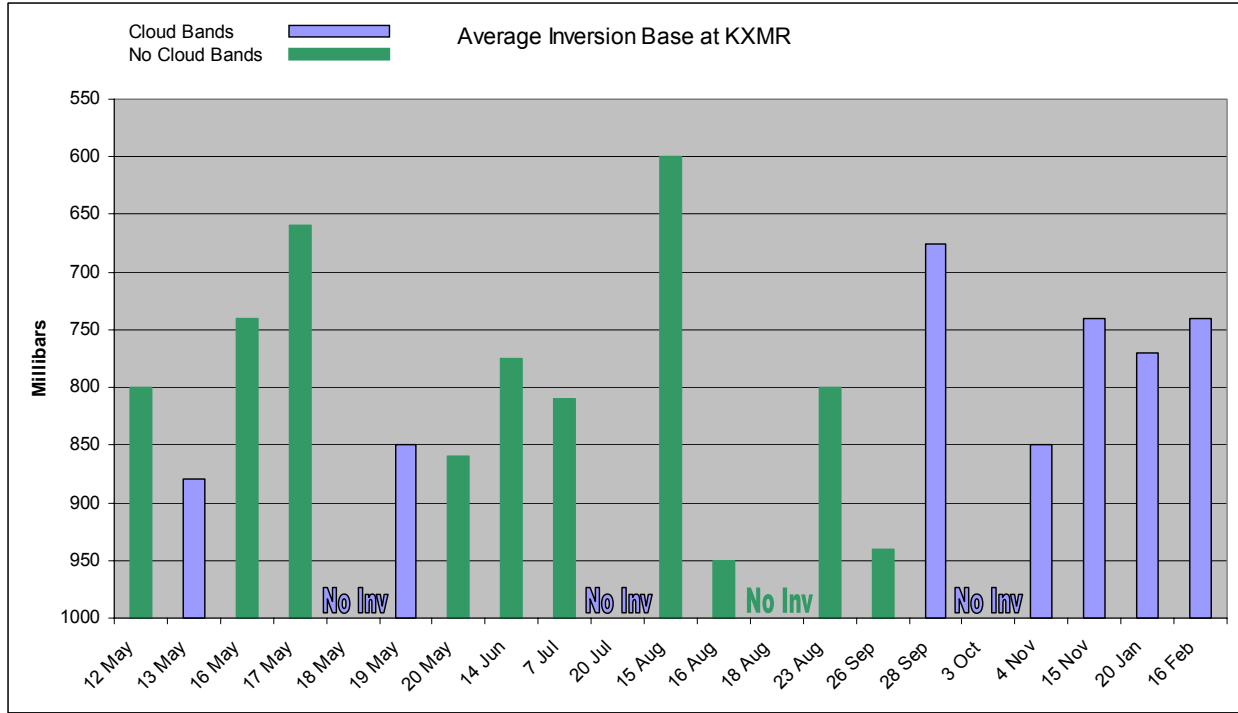


Figure 8. The average height (mb) of the inversion from morning soundings at XMR. If there was no inversion, the text “No Inv” is displayed. The light blue columns represent days when cloud bands reached the shore and the green columns represent days when the cloud bands were not present or did not reach the shore.

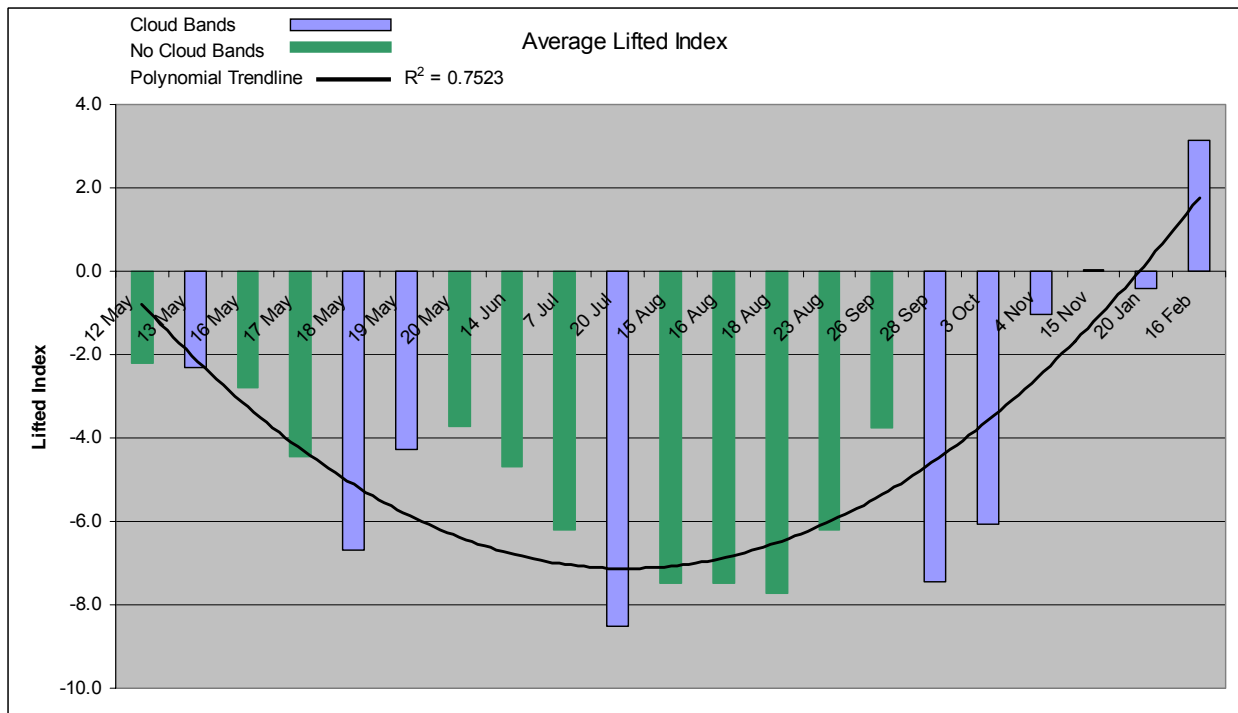


Figure 9. The average Lifted Index from morning soundings at MYNN, MFL and XMR. The light blue columns represent days when cloud bands reached the shore and the green columns represent days when the cloud bands were not present or did not reach the shore. The solid black line is the second order polynomial trend line.

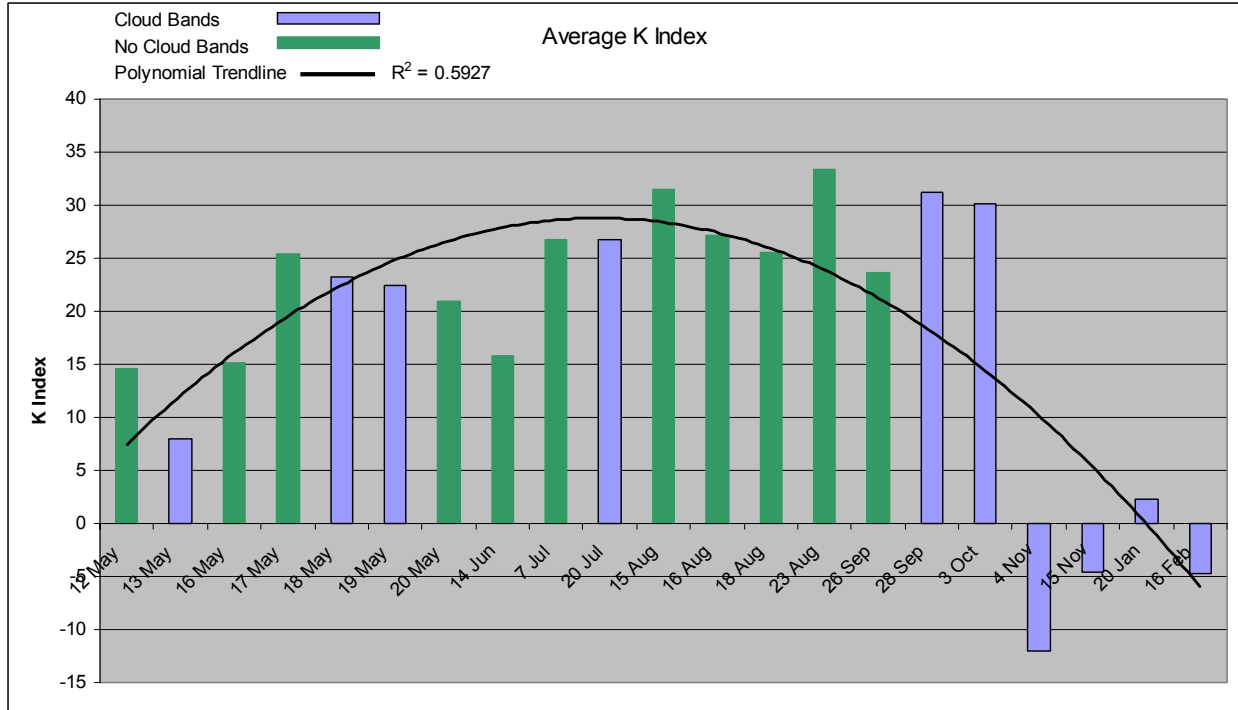


Figure 10. The average K Index from morning soundings at MYNN, MFL and XMR. The light blue columns represent days when cloud bands reached the shore and the green columns represent days when the cloud bands were not present or did not reach the shore. The solid black line is the second order polynomial trend line.

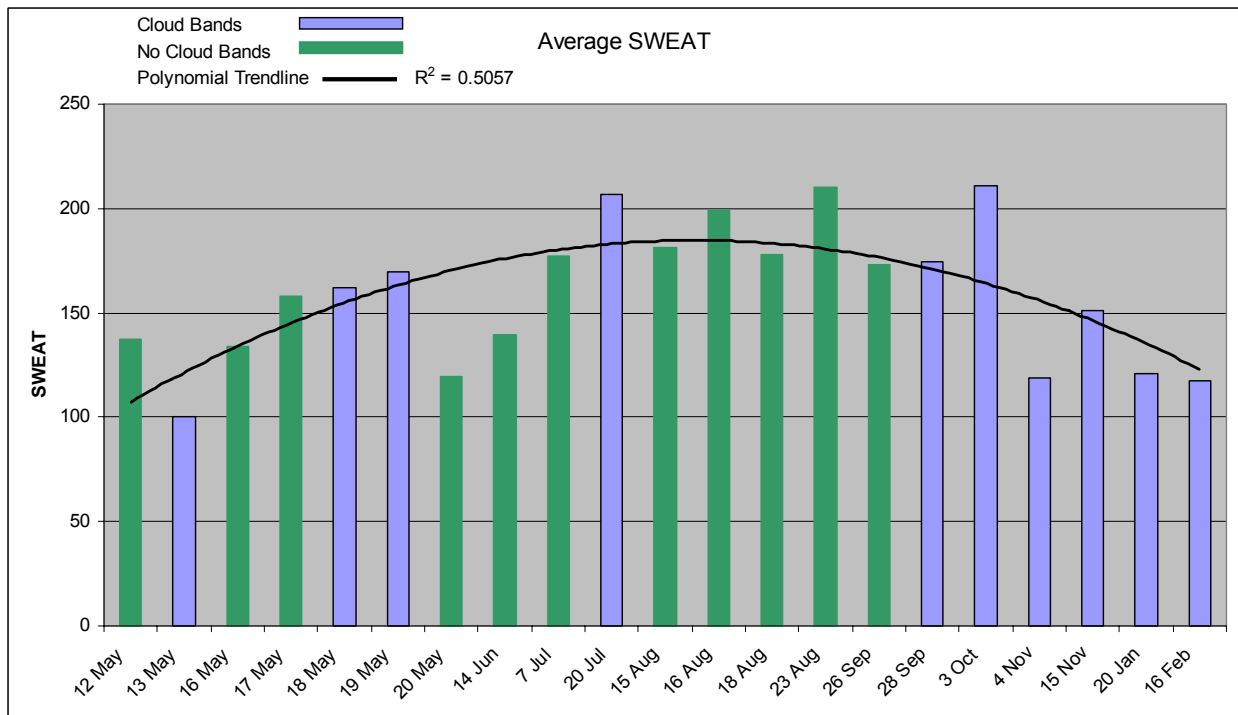


Figure 11. The average SWEAT from morning soundings at MYNN, MFL and XMR. The light blue columns represent days when cloud bands reached the shore and the green columns represent days when the cloud bands were not present or did not reach the shore. The solid black line is the second order polynomial trend line.

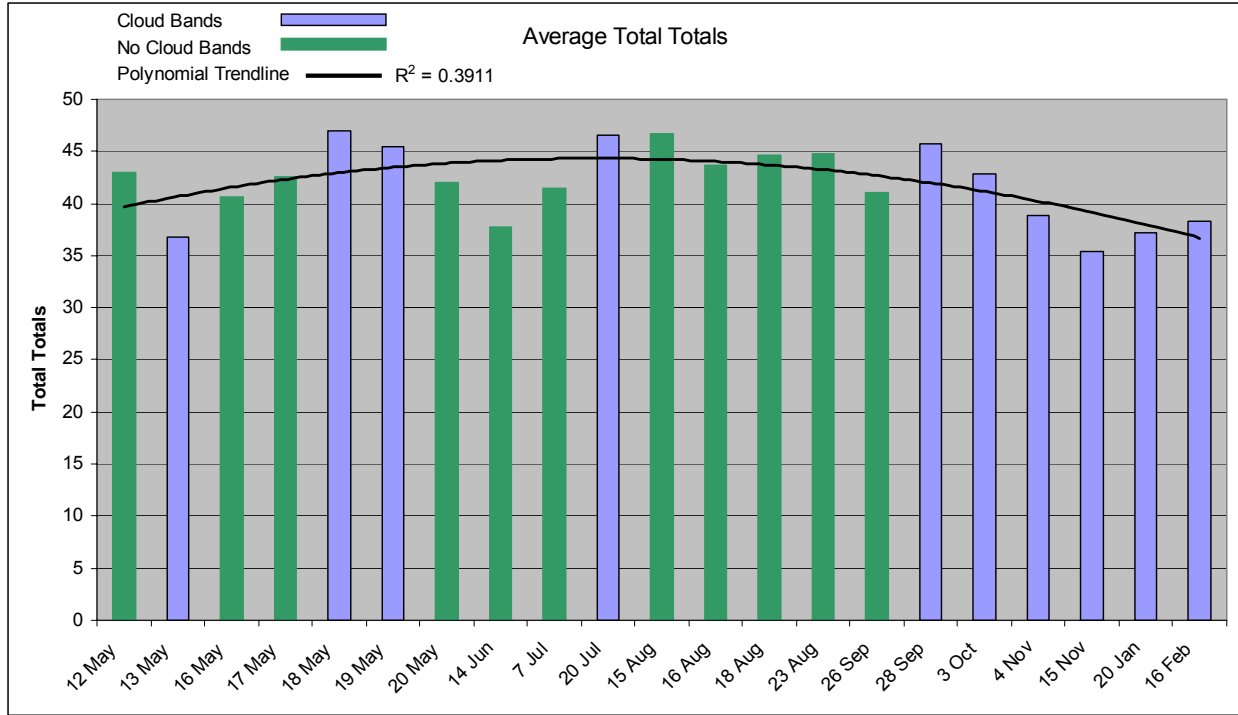


Figure 12. The average Total Totals from morning soundings at MYNN, MFL and XMR. The light blue columns represent days when cloud bands reached the shore and the green columns represent days when the cloud bands were not present or did not reach the shore. The solid black line is the second order polynomial trend line.

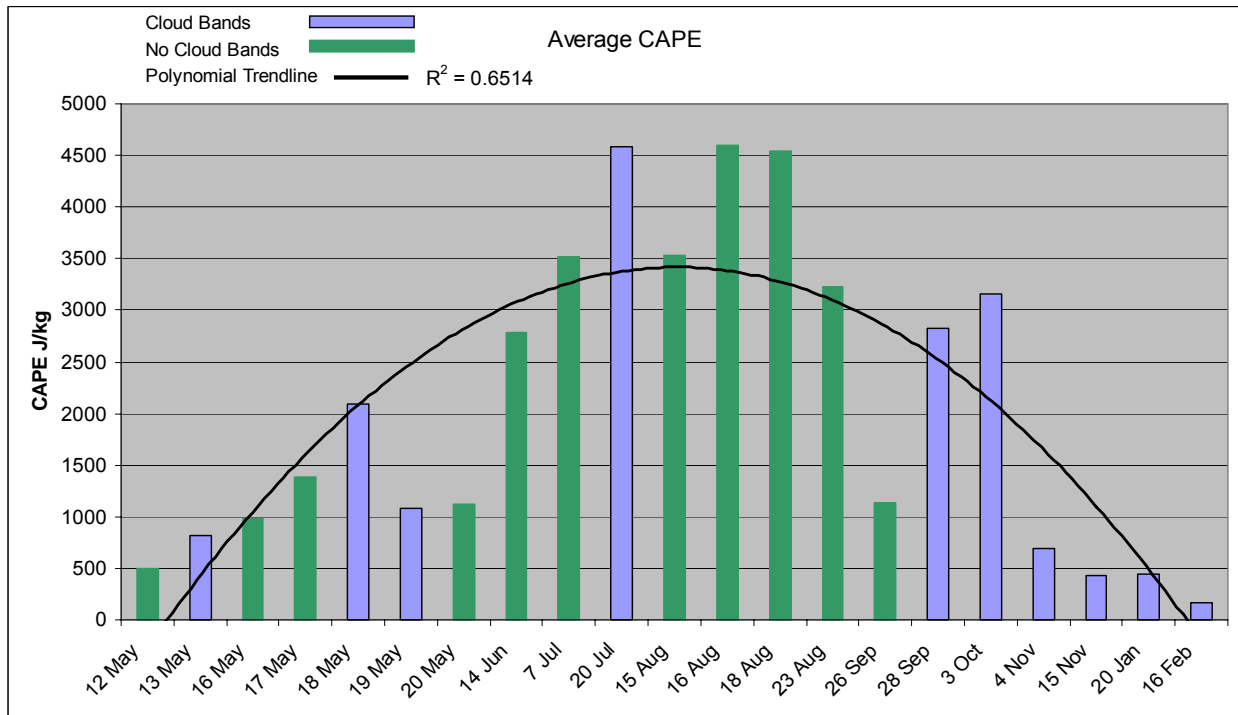


Figure 13. The average CAPE from morning soundings at MYNN, MFL and XMR. The light blue columns represent days when cloud bands reached the shore and the green columns represent days when the cloud bands were not present or did not reach the shore. The solid black line is the second order polynomial trend line.

3.2 Sea Surface Temperature (SST)

On most case days, the neither SST nor SST gradient appeared to have any influence on cloud band development, dissipation or movement. The AMU acquired SST data as image files from the Rutgers University Marine and Coastal Sciences web site (http://marine.rutgers.edu/cool/sat_data/) and the University of South Florida (USF) Institute for Remote Sensing web site (<http://imars.usf.edu/sst/>). The data from both sites were created from the National Oceanic and Atmospheric Administration's (NOAA) Polar Orbiting Environmental Satellite (POES) series. The Rutgers images (Figure 14) were built from single-pass Advanced Very High Resolution Radiometer (AVHRR) data while the USF images (Figure 15) were 3-day composites of AVHRR data. A composite is created to reduce cloud coverage contamination and is not quite the same as an average: if there is cloud coverage on one or more of the data points, that value is not used to compute the average. The USF composites were made with both day and night satellite imagery. They are also interactive and permit a user to select a point on the image to receive a display of the SST at that point. The AMU used this feature to analyze the SST just off the coast of CCAFS, in the Gulf Stream and to compute the difference in SST between the regions just offshore XMR and West End, Grand Bahama (MYGW).

The SST analyses did not show any obvious correlation to cloud band development or movement. The SST values offshore CCAFS (Figure 16) ranged from 62°F to 85°F and cloud bands moved onshore in this temperature range with no bias toward cool or warm water. The SST difference between XMR and MYGW as shown in Figure 17 ranged from near 0°F to 10°F. The SST offshore CCAFS was always equal to or less than the SST offshore MYGW. The Δ SST was generally larger in the winter; but it did not make a difference in cloud band development or movement onshore. Finally, cloud bands did not show favorable development in the vicinity of the Gulf Stream between XMR and MYGW as shown in Figure 18. A seasonal change in the maximum Gulf Stream SST is evident with a range of 76°F to 87°F but there is no significant correlation to cloud band development or movement.

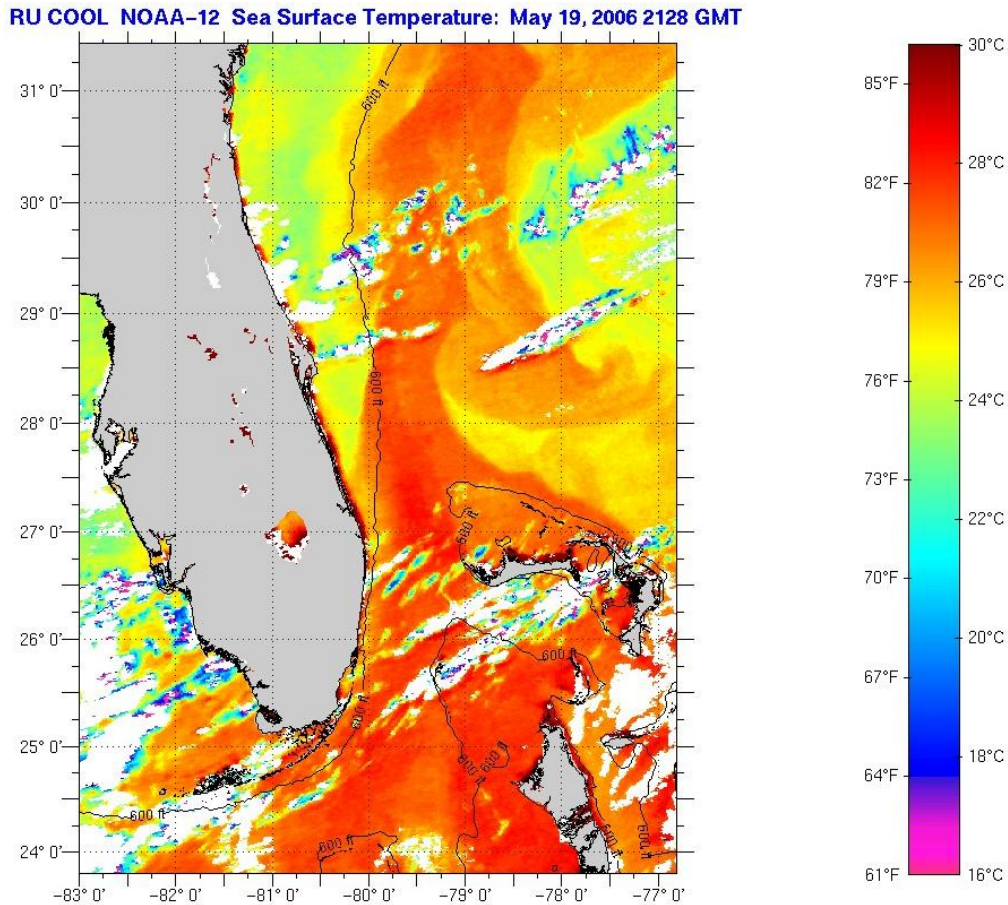


Figure 14. Example of the SST single pass image from the Rutgers University Marine and Coastal Sciences web site on 19 May 2006 at 2128 UTC from the NOAA-12 satellite.

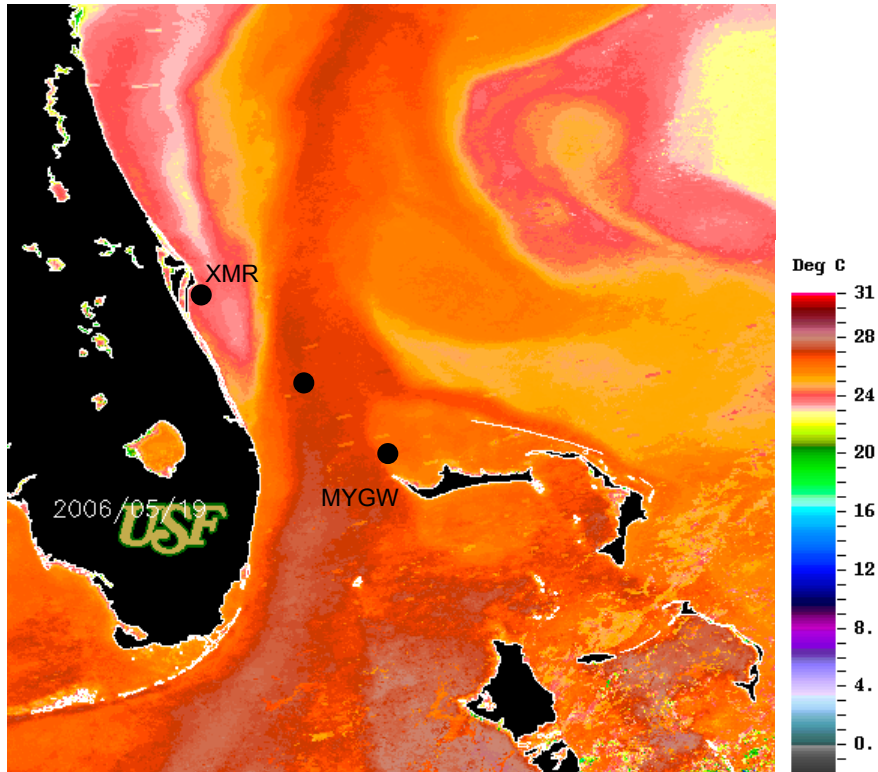


Figure 15. Example of a SST 3-day composite image from the USF Institute for Remote Sensing web site. The three solid black circles indicate the locations used in this study to retrieve SST for analysis. The date over the USF symbol is the middle of the three days 18-20 May 2006.

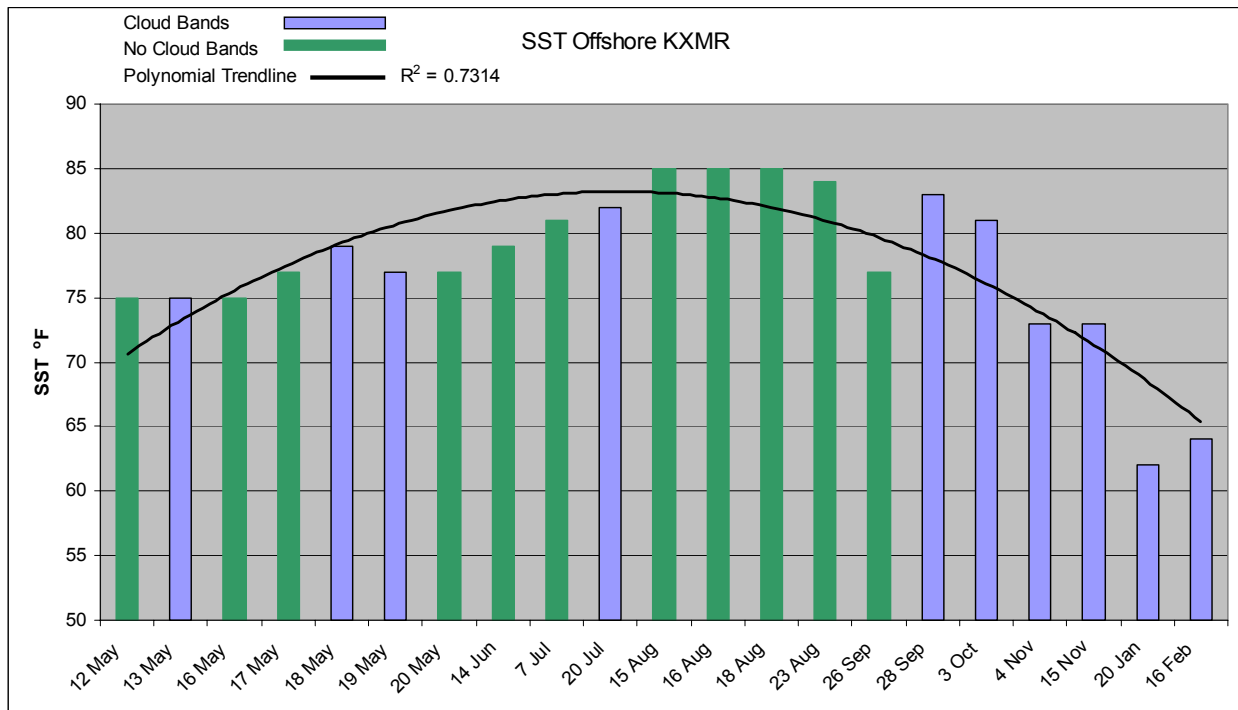


Figure 16. The SST values just offshore XMR on all the case study days. The light blue columns represent days when cloud bands reached the shore and the green columns represent days when the cloud bands were not present or did not reach the shore.

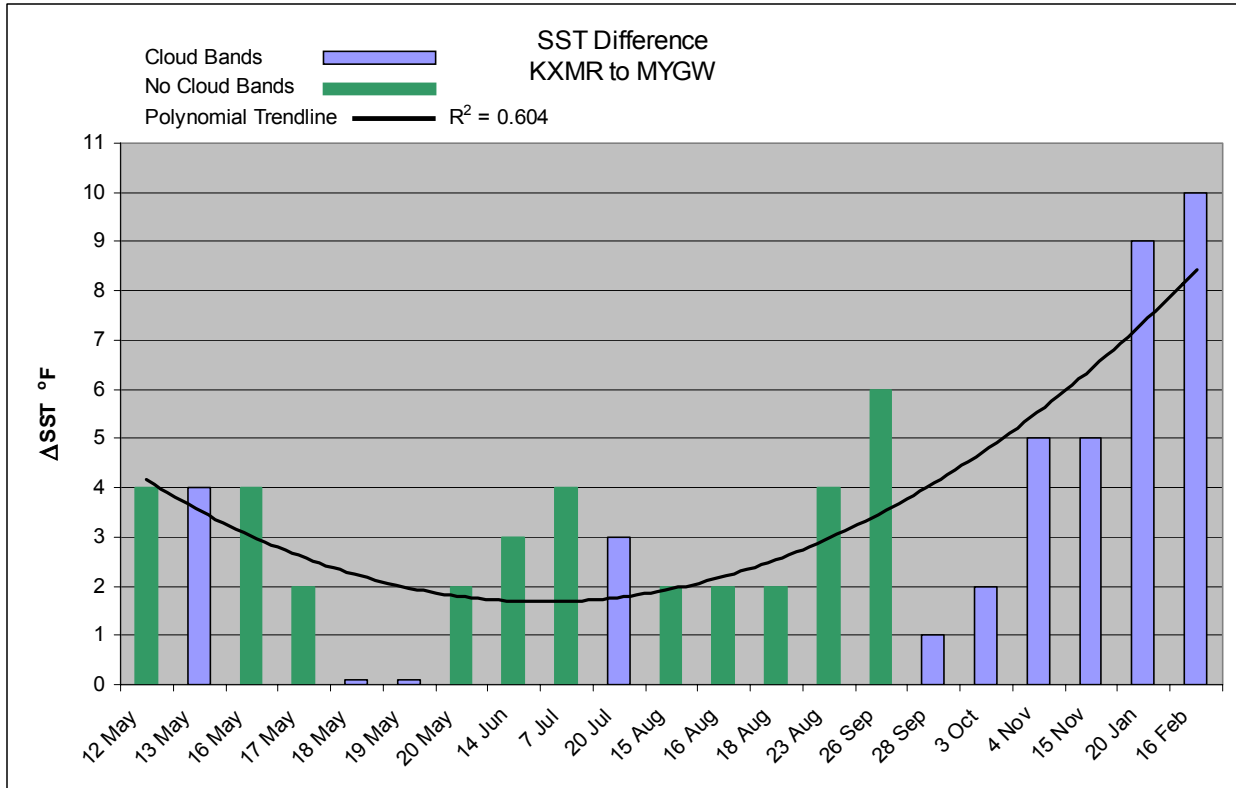


Figure 17. The SST differences on all the case study days between the region just offshore XMR and MYGW (see Figure 15). The light blue columns represent days when cloud bands reached the shore and the green columns represent days when the cloud bands were not present or did not reach the shore.

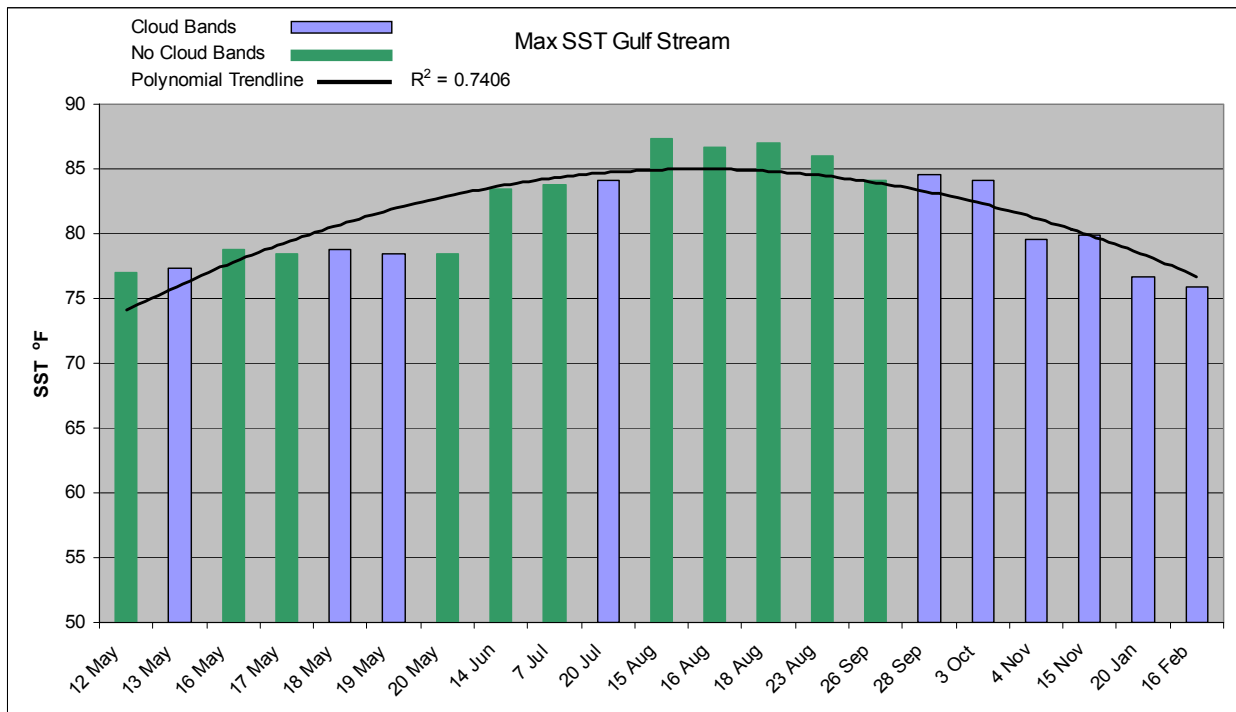


Figure 18. The maximum SST between XMR and MYGW (see Figure 15) on all the case study days. The light blue columns represent days when cloud bands reached the shore and the green columns represent days when the cloud bands were not present or did not reach the shore.

3.3 Low-level Phenomena

One factor related to cloud band development and movement onshore was the median wind speed in the surface to 700 mb layer. This layer was chosen based on observing the cloud band motion in visible satellite imagery and correlating the motion to low-level layer-averaged winds. Other layers considered were surface to 925 mb, surface to 850 mb and surface to 500 mb but the surface to 700 mb layer-averaged winds displayed the best fit to the cloud band motion on most days in the data set. For all valid easterly flow days examined, the median wind speed in this layer on days when the cloud bands reached the Florida shore was 9 knots while on days when the cloud bands were not present or did not reach the shore the median wind speed was 3 knots (Figure 19). For the latter case, examination of visible satellite imagery showed that cloud bands well offshore tended to develop and dissipate faster than the weak low-level winds could advect them. If the cloud bands developed very close to the coast (not frequently observed in this data set) they could make it onshore during weak low-level wind situations.

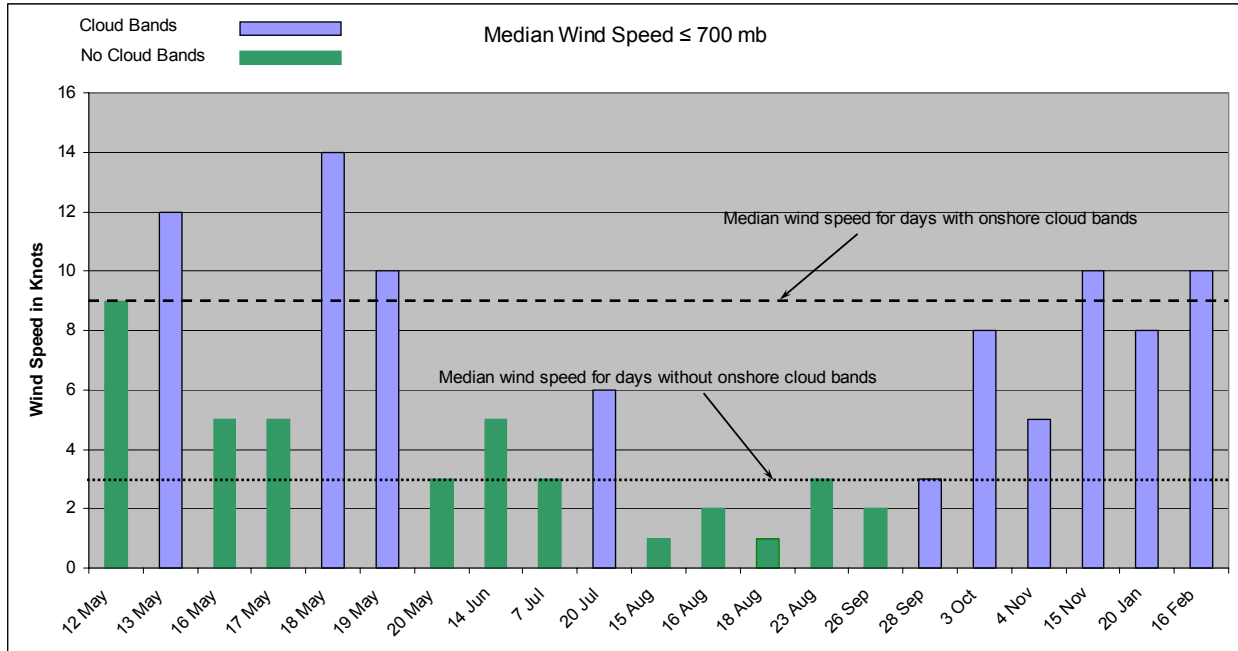


Figure 19. The average wind speed in the layer from surface to 700 mb from XMR. The light blue columns represent days when cloud bands reached the Florida shore and the green columns represent days when the cloud bands were not present or did not reach the shore.

In addition to the impact of the low-level layer average wind speed, the location and curvature of the flow around the low-level high pressure ridge proved to be another important factor in cloud band movement. Figure 20 illustrates an example of how the location of the low-level high pressure ridge and curvature of the flow around the high influence movement of cloud bands. It shows the 16 August 2005 RUC 6-hour layer average wind field forecast from 1000 – 700 mb valid at 21 UTC superimposed on a GOES visible satellite image at 1815 UTC. The low-level high pressure area is centered east of northern Florida and the high pressure ridge extends westward to north of JAX. Analysis of visible satellite image loops for this day showed the cloud bands in the vicinity of The Bahamas moving west while the cloud bands offshore XMR initially moved north-northwest then north and eventually northeast by the time they were north of JAX. The cloud bands immediately offshore XMR moved parallel to the coast near KSC/CCAFS and, on this day, also dissipated rapidly in the weak flow.

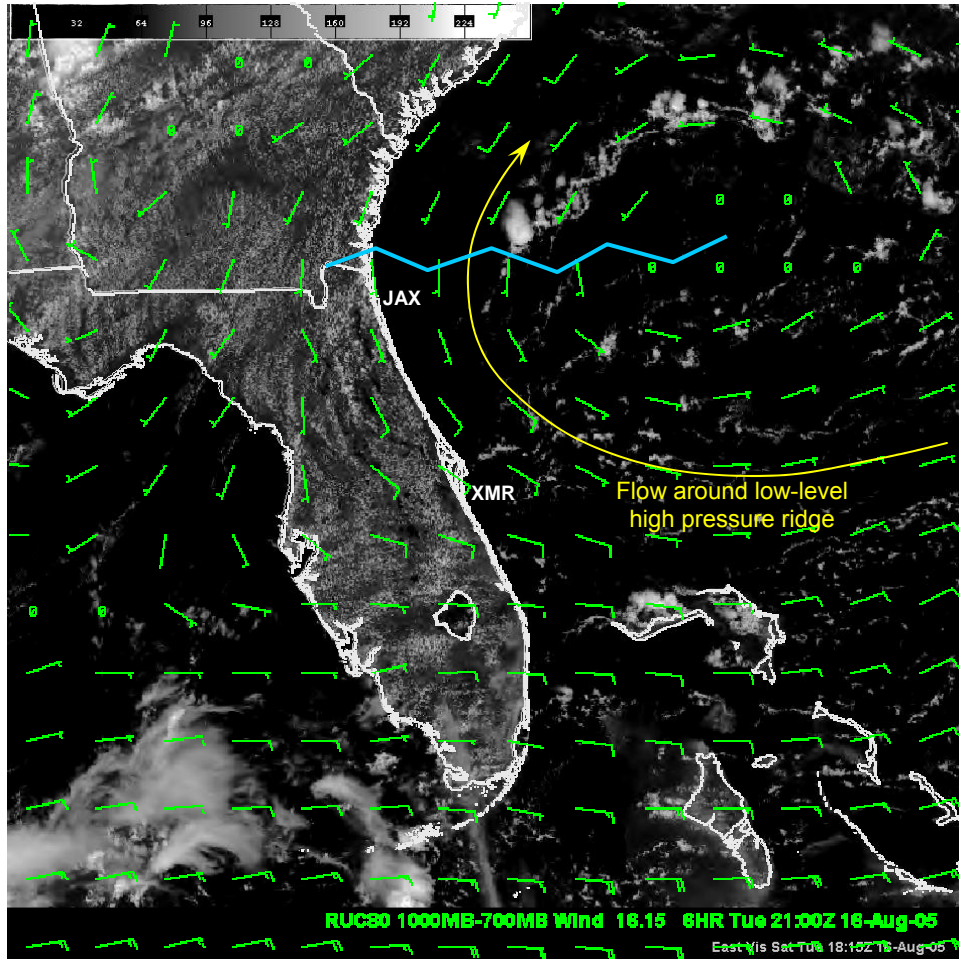


Figure 20. The RUC 6-hour layer average 1000 mb – 700 mb wind forecast valid 21 UTC superimposed on the visible satellite image on 16 August 2005 at 1815 UTC from the GOES East satellite. The yellow arrow represents the wind flow around the low-level high pressure area. The low-level high pressure ridge position is shown by the solid blue jagged line.

3.4 Upper-level Phenomena

The AMU investigated upper-level phenomena including vertical wind directional change, jet streaks, temperature gradients, and average wind speed and direction in various layers. In this dataset, there was very little correlation with cloud band development and maintenance related to upper-level phenomena. However, there were some subtle signatures noted which will be addressed in this section.

On days with cloud band formation, the winds in the XMR sounding tended to veer slightly with height at or below 700 mb with no backing or veering above this level. On days with no cloud bands, the winds at or below 700 mb showed little to no directional change but above 700 mb the winds generally backed. More notable, cloud bands were more prevalent with low-level easterly flow and westerly flow at or above 500 mb. With deep easterlies (surface to 100 mb), cloud bands only formed and made it onshore on one of the case days.

The AMU also examined jet streaks in the 300 – 100 mb range. Using the Uccellini jet streak model (Uccellini and Kocin 1987), the ageostrophic motions and divergence/convergence at jet streak level are shown in Figure 21. In the KSC/CCAFS area, especially during the warm season, what appears to be a weak 20-40 knot jet streak could be high enough relative to the surrounding winds at jet stream levels to create similar divergent and convergence regions. Using 40 km RUC model and 4 km ARPS output, the AMU determined that the right jet exit region or left jet entrance region appeared to suppress convection and cloud band development. However, on days when the right jet entrance region or left jet exit region was evident, cloud band development was not always enhanced. Figure 22

shows a visible satellite image from 20 May 2005 at 1745 UTC, one of the easterly flow days in this data set. The 250 mb wind barbs, isotachs and an arrow representing the jet core are overlaid on the satellite image in Figure 22a. For clarity, Figure 22b only shows the jet core arrow and labels corresponding to the left entrance and right entrance regions of the jet streak. The clouds were suppressed in the vicinity of the left entrance region, as well as the KSC/CCAFS area, as predicted by the Uccellini jet streak model. In the right entrance region, clouds were widespread as they developed in the region of upper level divergence.

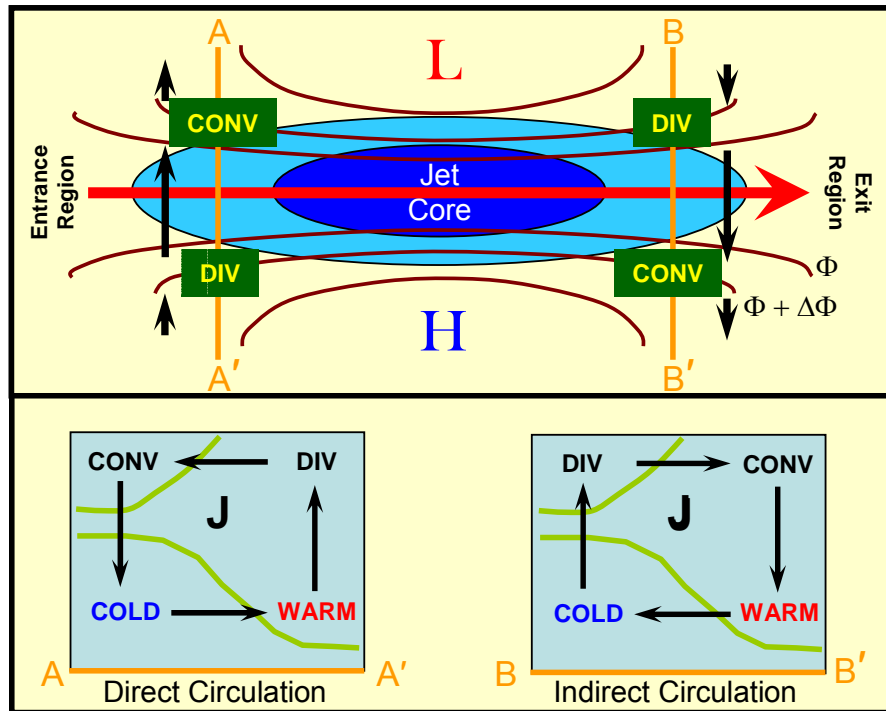


Figure 21. The Uccellini four quadrant straight jet streak model showing the ageostrophic horizontal and vertical motions (Uccellini and Kocin 1987).

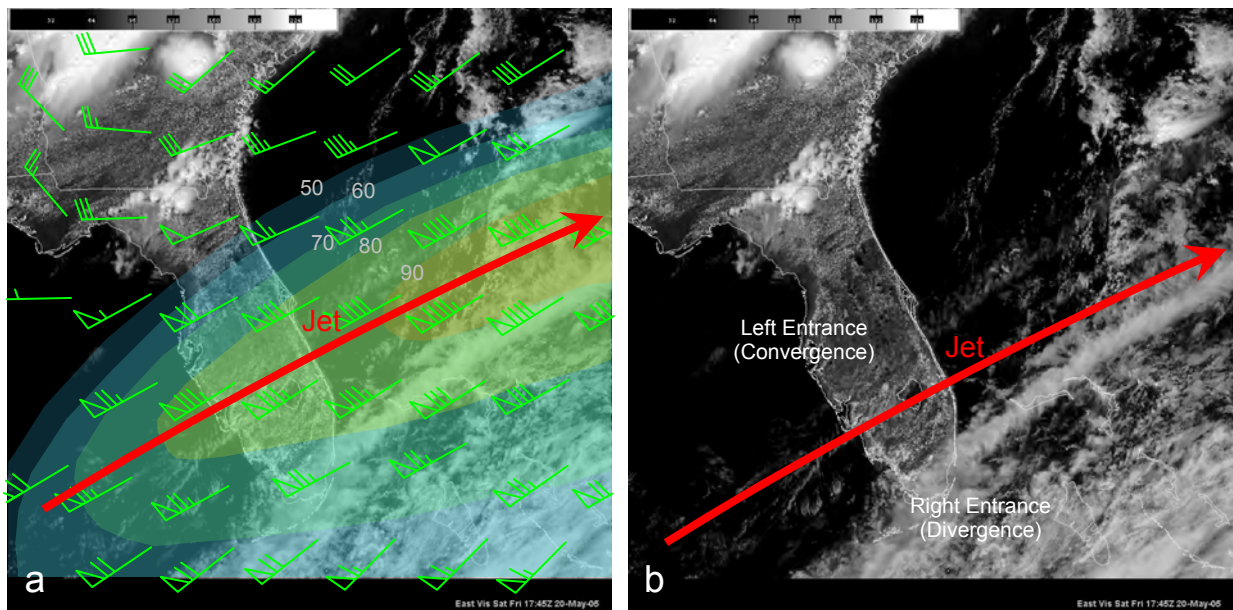


Figure 22. Visible satellite image on 20 May 2005 at 1745 UTC with (a) 250 mb wind barbs and isotachs (isotachs are shaded at 50, 60, 70, 80 and 90 knots) from the Eta 6 hour forecast valid at 1800 UTC overlaid and (b) the center line of the 250 mb jet and the jet left and right entrance regions from (a) depicted for clarity.

3.5 Sea Breeze Effect

The visible satellite imagery collected during this task was used to identify the motion and development of the convergence cloud bands. During the analysis portion of the task, the AMU noticed certain days when cloud bands were moving towards the coastline and dissipating at various distances offshore before crossing the coast. Upon examination of the visible satellite loops with overlaid data such as surface observations, low-level streamlines and 250 mb winds, it became evident that the cloud bands moved onshore and did not dissipate when a sea breeze was not present or well inland, but they did dissipate in the wake of a sea breeze front that was generally east of the middle of the peninsula presumably due to post sea breeze front subsidence. However, on some days when upper level jet support was present and strong enough to oppose the sea breeze subsidence, the clouds did not dissipate behind the sea breeze front.

An example of clouds dissipating behind the sea breeze front but maintaining their structure before the sea breeze front formed is shown in Figure 23 which shows a series of four visible satellite images from 16 August 2005. The surface observations and low-level streamlines were overlaid on the satellite images in (a) and (b) and the position of the sea breeze front was added in (c) and (d). In (a) and (b), clouds over the Atlantic Ocean were moving westward toward Florida and continued to move across the coastline over land. The east coast sea breeze front was not visible at these times. The low-level high pressure ridge extended from the Atlantic Ocean westward to central Florida. South Florida was under the influence of easterly flow, central Florida was experiencing southeasterly flow and in north Florida the flow was southwesterly. In south Florida, the east coast sea breeze front was never observed as low clouds moved from the water across the coast and then across southern Florida throughout the entire day. As the east coast sea breeze front developed and moved inland over central Florida, low clouds moving westward over the ocean began to dissipate as they reached the sinking air east of the sea breeze front. As the sea breeze front continued to move westward into central Florida, skies cleared on the east side of the front over the land.

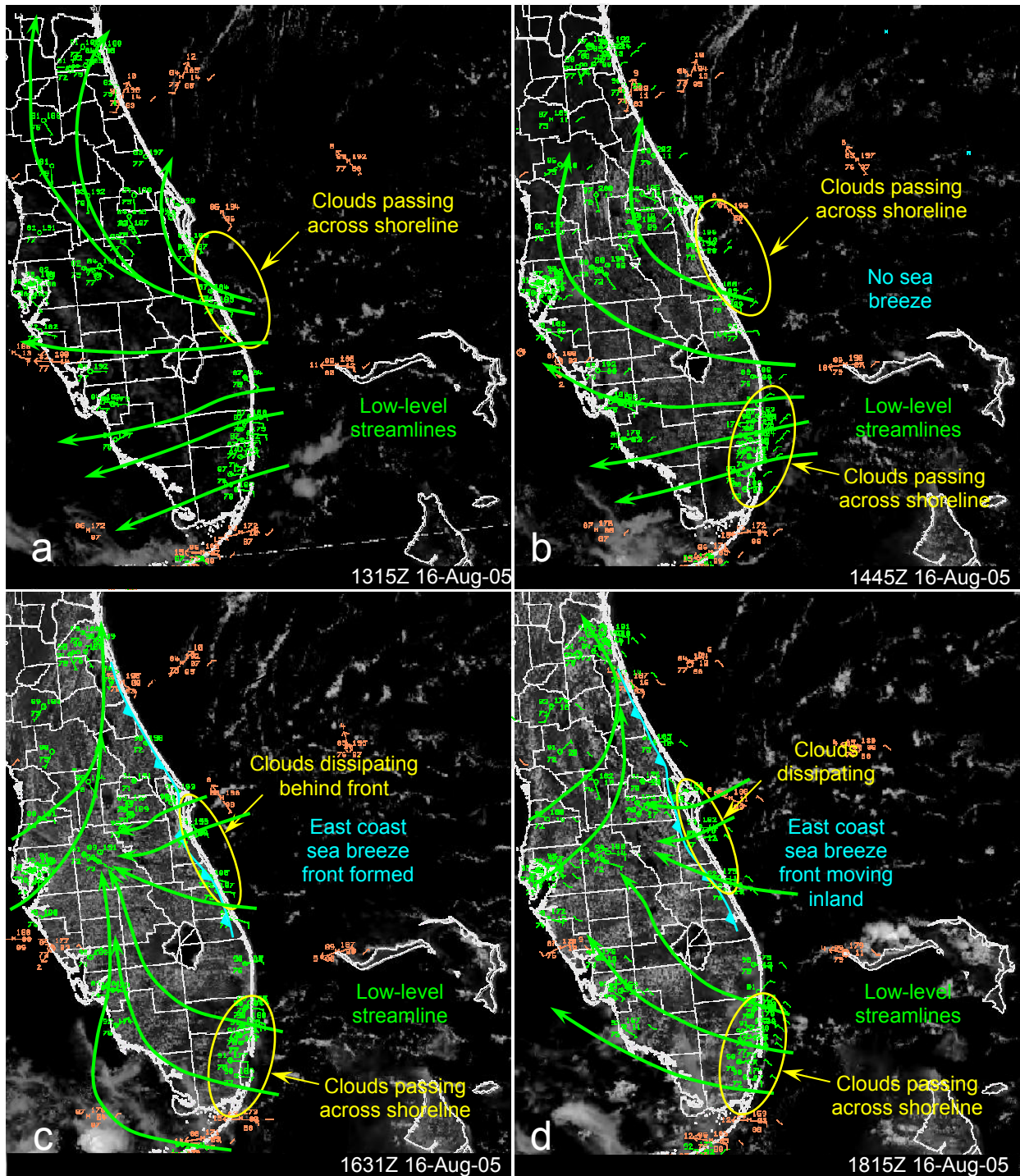


Figure 23. Visible satellite images on 16 August 2005 at (a) 1315 UTC with surface observations and low-level streamlines overlaid, (b) 1445 UTC with surface observations and low-level streamlines overlaid, (c) 1631 UTC with surface observations, low-level streamlines overlaid and the position of the sea breeze front overlaid and (d) 1815 UTC with surface observations, low-level streamlines and the position of the sea breeze front overlaid.

4 Individual Case Studies

This section presents two examples from the easterly flow case days used in this task. The first example is from a day when convergence cloud bands developed and moved onshore KSC/CCAFS, and the second example illustrates a day when they did not form.

4.1 Convergence Cloud Band Day – 20 July 2005

Convergence cloud bands could be seen offshore in the early morning visible satellite images and then advected onshore near KSC/CCAFS during the late morning and early afternoon. The visible satellite image at 1540 UTC (Figure 24) shows that there were a number of large areas of low-level clouds in the Atlantic Ocean. The Eta surface wind and streamline analysis at 1200 UTC is overlaid on the satellite image in Figure 24 to show the general low-level wind flow and low-level high pressure ridge position just north of JAX. The cloud bands from Daytona Beach (DAB) southward were moving westerly (onshore) while the cloud bands north of DAB were moving north-northeasterly. Some of the cloud bands east of central Florida were precipitating as can be seen in the NWS MLB WSR-88D 0.5° radar reflectivity image in Figure 25. Not all of the precipitating cloud bands made it onshore and those that did were generally south of KSC/CCAFS. The non-precipitating cloud bands did make it onshore near KSC/CCAFS and brought with them broken to overcast conditions at the Shuttle Landing Facility later in the day.

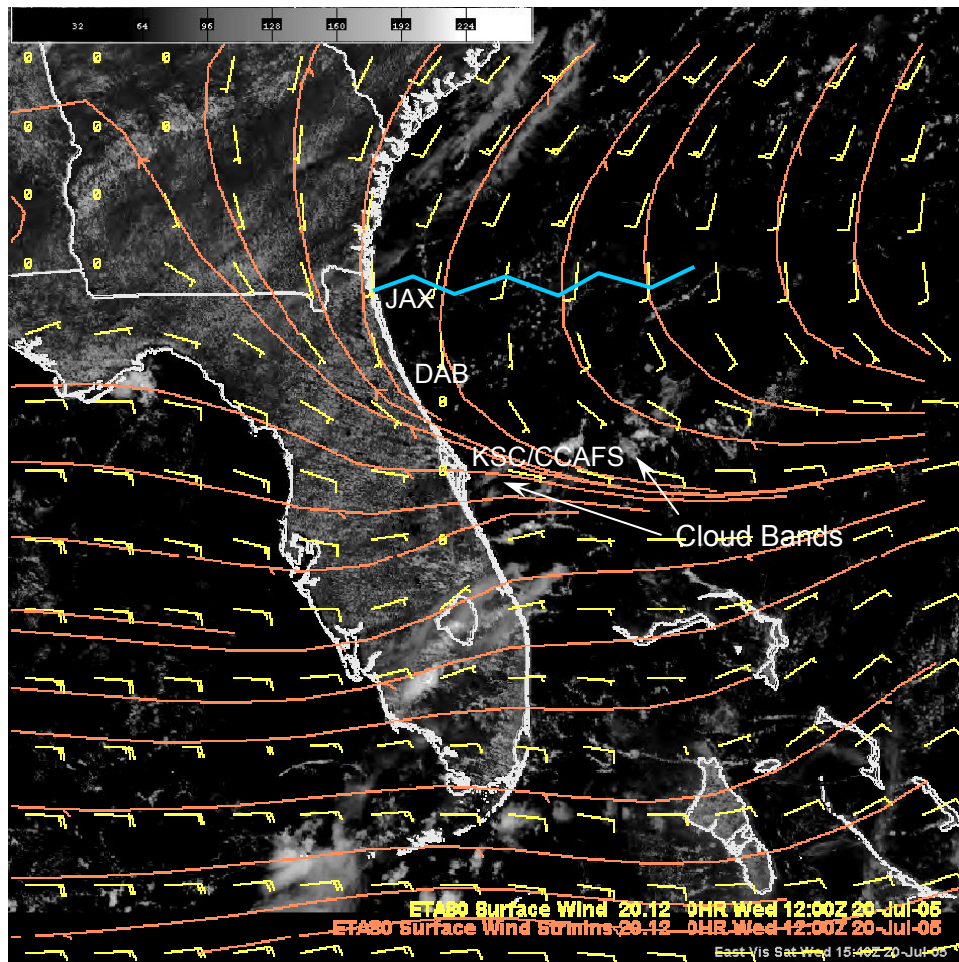


Figure 24. Visible satellite image on 20 July 2005 at 1540 UTC from the GOES East satellite. The Eta surface wind and streamline analysis at 1200 UTC is overlaid on the satellite image. The wind barbs are plotted in yellow and speed is in knots. The streamlines are depicted by the solid orange lines. The low-level high pressure ridge position is shown by the solid blue line near JAX.

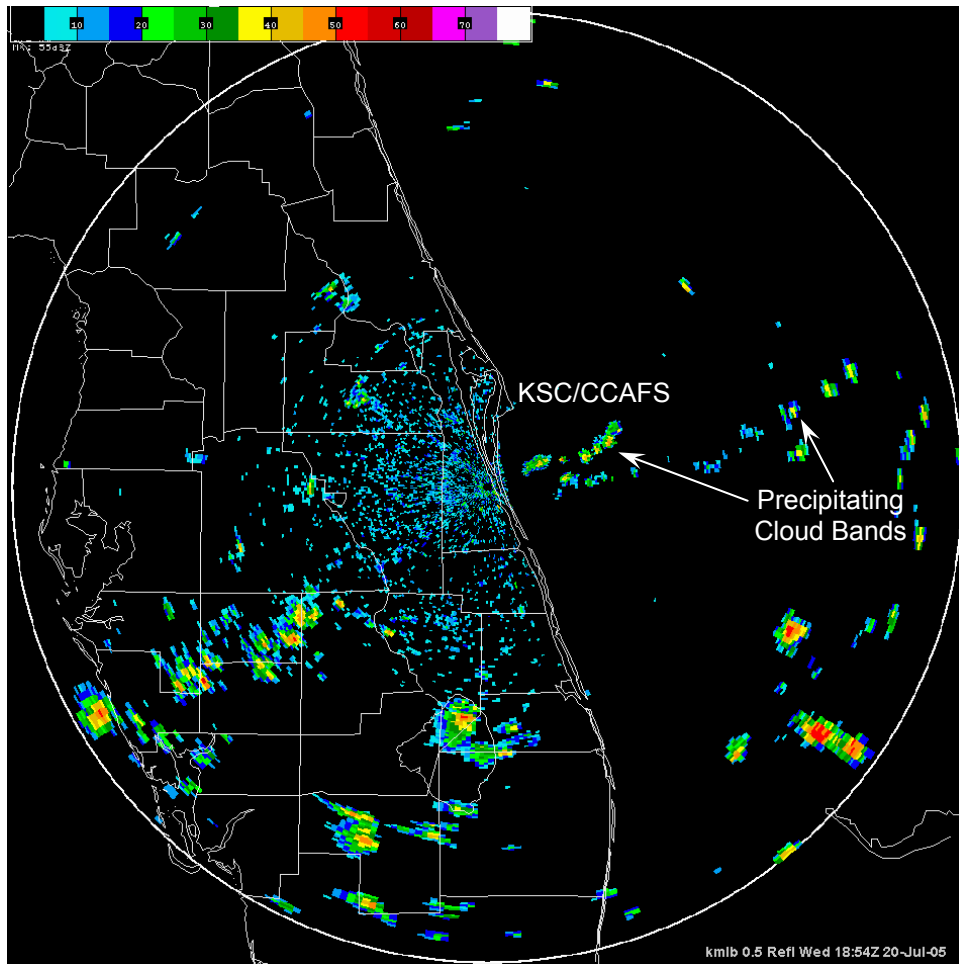


Figure 25. The 0.5° reflectivity image from the NWS MLB WSR-88D radar on 20 July 2005 at 1854 UTC. Precipitating cloud bands can be seen southeast of KSC/CAAFS with reflectivity values up to 45 dBZ.

4.1.1 Analysis of Low-level Features

The low-level high pressure ridge extended westward from well offshore in the Atlantic Ocean to near JAX (Figure 24). The prevailing wind direction along the east central Florida coast from surface to 700 mb was south of east at 105° with an average wind speed of ~6 knots. The average wind speed in the layer from surface to 700 mb was a factor in whether or not the cloud bands reached the shore in this case. As discussed in Section 3.3 and shown in Figure 19, the average wind speed in the layer on days when the cloud bands reached the shore was 8.6 knots while on days when the cloud bands were not present or did not reach the shore the average wind speed was 3.5 knots.

The location and curvature of the flow around the low-level high pressure ridge proved to be an important factor in cloud band movement in this case. As seen in the streamline depiction in Figure 24, there was a fairly long easterly fetch around the south side of the high pressure ridge from just north of KSC/CAAFS south through the Caribbean region. The cloud bands in the long easterly fetch were advected onshore over the Florida peninsula from KSC/CAAFS southward while the cloud bands seen later in the day at 1902 UTC east-northeast of JAX in Figure 26 were moving away from the coast toward the northeast.

The visible satellite image loops revealed the cloud bands moved approximately parallel to the low-level streamlines. Therefore, when the low-level ridge in the Atlantic is north of KSC/CAAFS, it is more likely that cloud bands will move toward the shore. The visible satellite image loops also revealed the east coast sea breeze front was active on 20 July and by 1902 UTC (Figure 26) was positioned about one-fourth of the way inland along the Florida peninsula moving westward. As mentioned previously, cloud bands tended to dissipate in the wake of the sea breeze

front – but not on 20 July. The AMU believes this is because there was strong enough upper level support in the form of an easterly jet streak at 250 mb as shown in Figure 27.

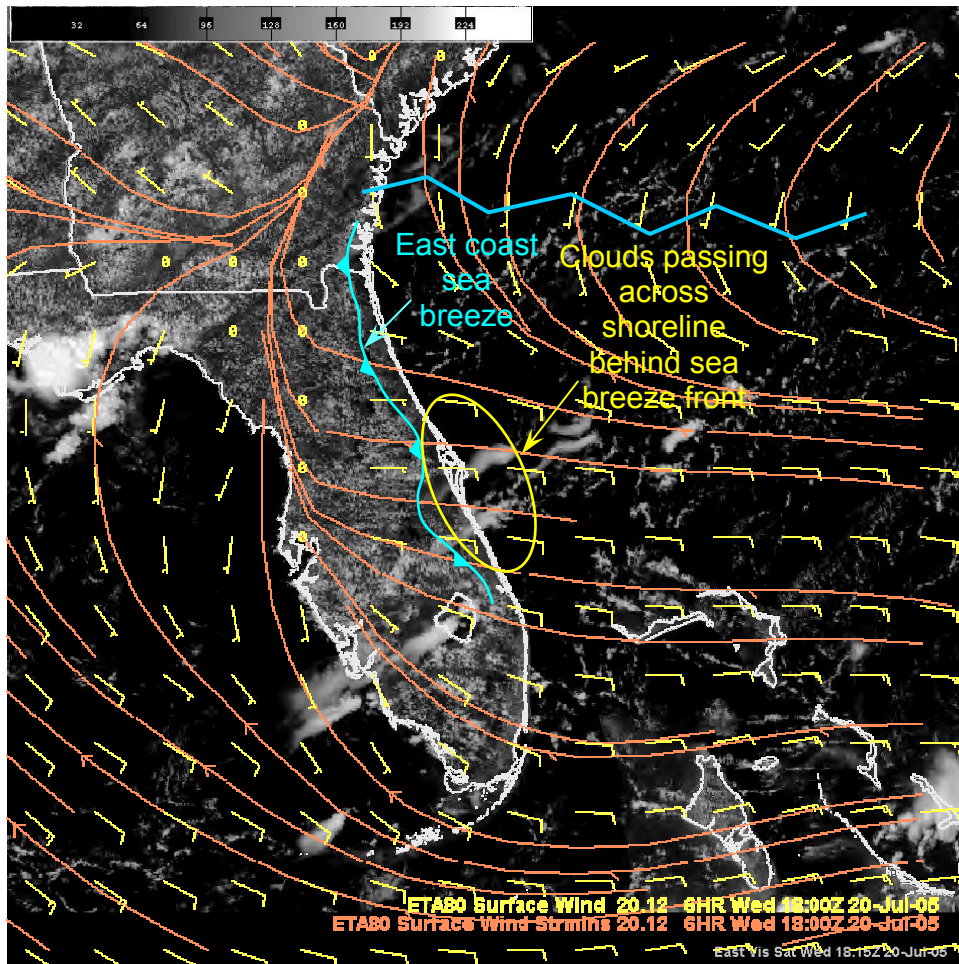


Figure 26. Eta 6-hour surface wind and streamline forecast valid 20 July 2005 at 1800 UTC as in Figure 24. The Eta data is superimposed on the visible satellite image on 20 July 2005 at 1815 UTC.

4.1.2 Analysis of Upper-level Features

An easterly 55 knot jet streak at 250 mb moved from northeast to southwest across south central Florida during the day. East central Florida was under the influence of the right entrance region of the jet streak which may have produced enough upper level divergence to counteract the sea breeze front subsidence region and, therefore, allowed the cloud bands to persist and move onshore behind the sea breeze front. Figure 27 shows the position of the Eta 6-hour forecast of the 250 mb jet streak valid 20 July 2005 at 1800 UTC overlaid on the visible satellite image at 1815 UTC. The position of the east coast sea breeze front, jet streak position and jet right and left entrance regions are identified. Cloud bands and convection can be seen in the vicinity of KSC/CCAFS whereas southeast Florida was generally cloud band free under the left entrance regions of the jet streak. By about 1900 UTC, thunderstorms developed west-northwest of The Bahamas as the jet streak moved away from the Florida peninsula.

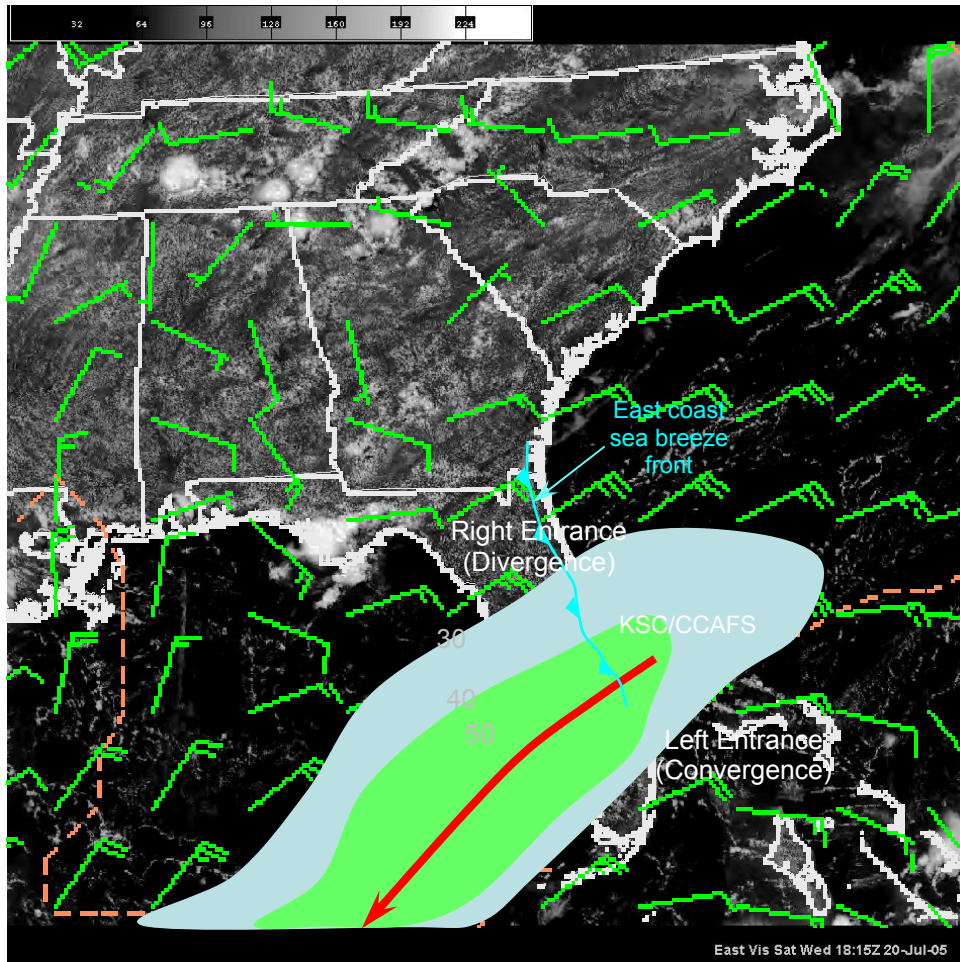


Figure 27. Eta 6-hour 250 mb wind forecast valid 20 July 2005 at 1800 UTC. Wind barbs are in green and knots. Isotachs are shaded at 30, 40 and 50 knots. The Eta data is superimposed on the visible satellite image on 20 July 2005 at 1815 UTC. The position of the east coast sea breeze front is shown in cyan.

4.2 No Convergence Cloud Band Formation – 16 May 2005

Convergence cloud bands could be seen well offshore in the visible satellite image on 16 May 2005 at 1745 UTC (see Figure 28). The Eta surface forecast streamline analysis valid at 1800 UTC is overlaid on the satellite image to show the general low-level wind flow and low-level high pressure ridge position over KSC/CAFS and extending westward. Due to the low-level high pressure ridge position and curvature of the wind flow around the ridge, the low-level winds were south-southeasterly and nearly parallel to the east central Florida coastline and the cloud bands moved slowly north-northwestward.

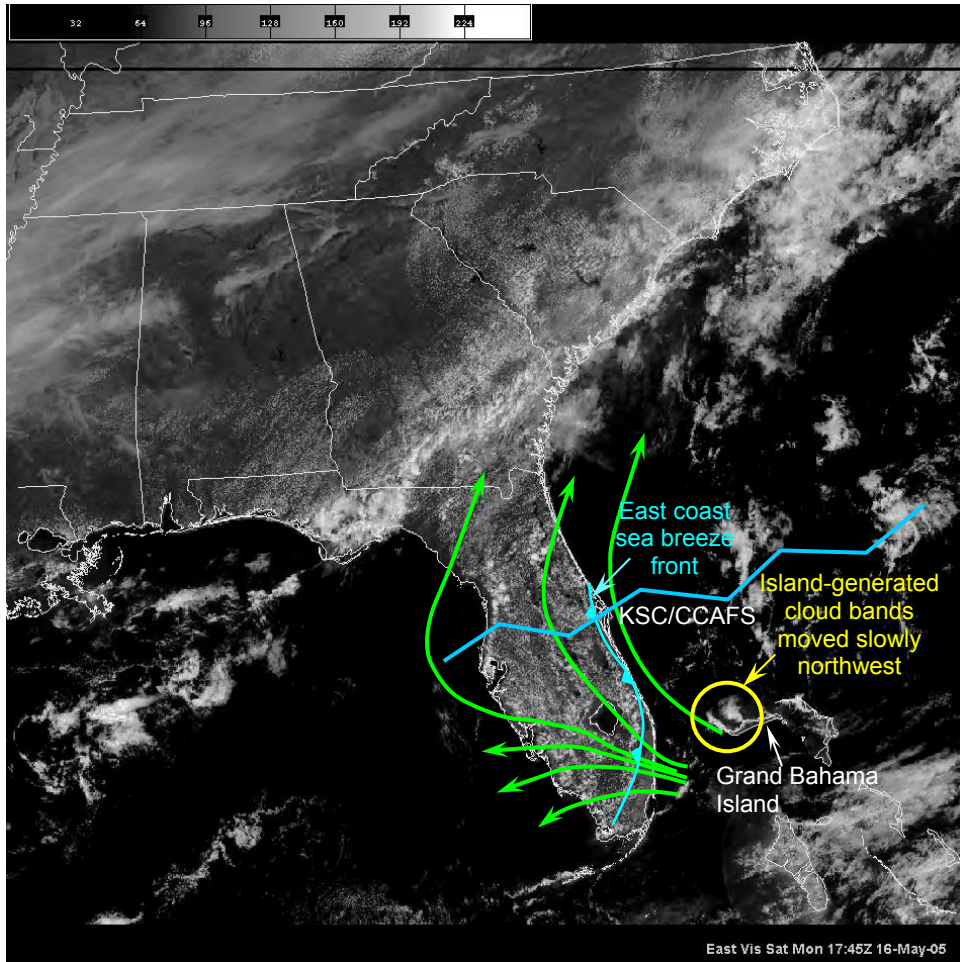


Figure 28. Visible satellite image on 16 May 2005 at 1745 UTC from the GOES East satellite. The Eta 6-hour forecast surface streamline analysis at 1800 UTC is overlaid on the satellite image as the green solid lines with arrows. The low-level high pressure ridge position is shown by the solid blue line. The position of the east coast sea breeze front is shown in cyan. Convergence cloud bands can be seen in the Atlantic Ocean east of southeast Florida and extending northwest from Grand Bahama Island.

4.2.1 Analysis of Low-level Features

The prevailing wind direction along the east central Florida coast in the layer from surface to 700 mb was variable with an average wind speed of about 5 knots. This is consistent with other days that did not have cloud band movement onshore. The morning soundings along the Florida east coast from MFL to XMR to JAX indicate the weak low-level flow was southeasterly at MFL (Figure 29), southerly near the surface then backing to northeasterly above 850 mb at XMR (Figure 30) and southwesterly at JAX (Figure 31). Based on the sounding data and the surface streamline analysis in Figure 28, the low-level high pressure ridge extended from well offshore in the Atlantic Ocean to near XMR as indicated by the solid blue line in Figure 28.

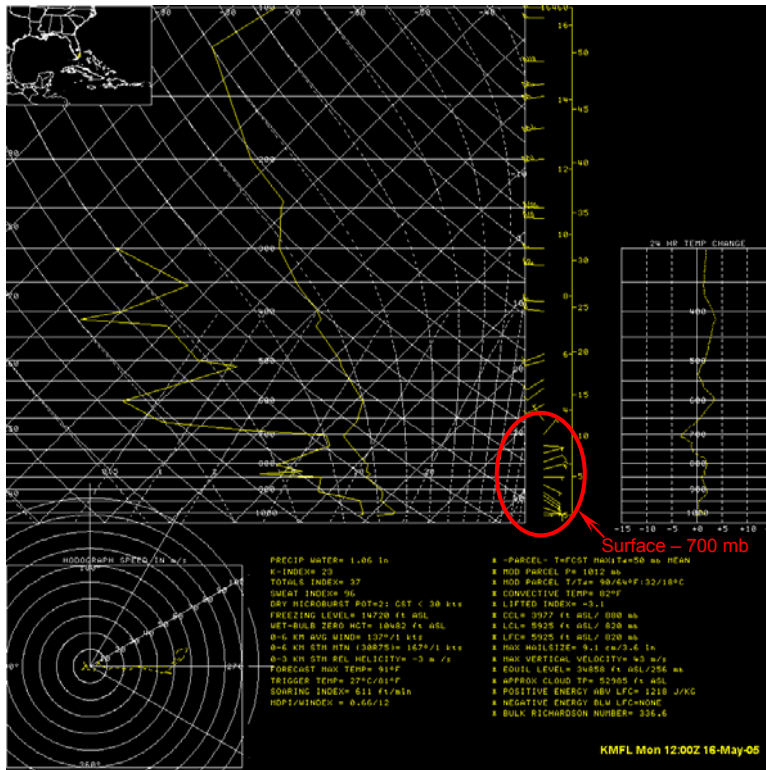


Figure 29. MFL sounding on 16 May 2005 at 1200 UTC. Vertical wind profile from surface to 700 mb is shown inside the red ellipse.

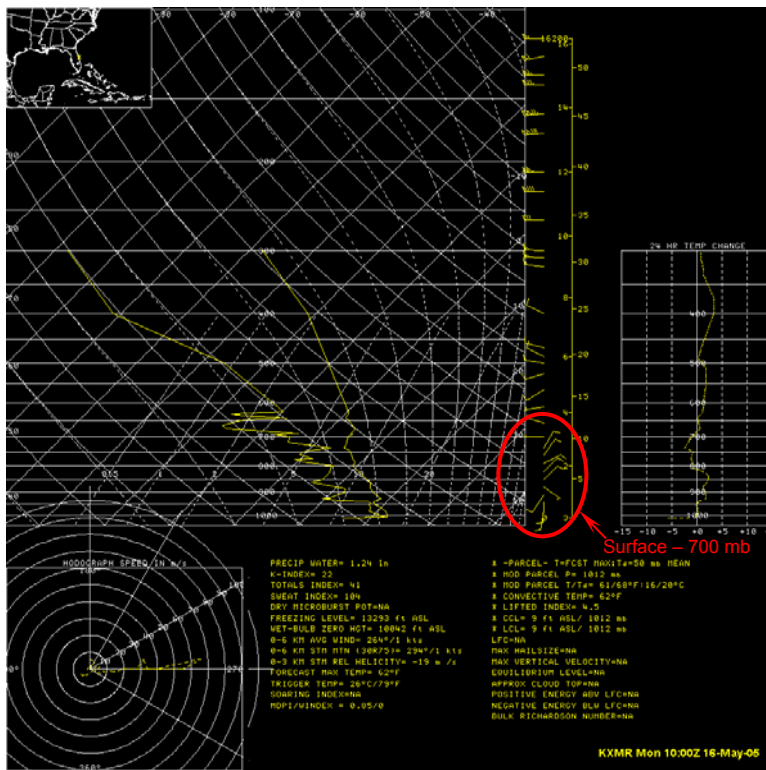


Figure 30. XMR sounding on 16 May 2005 at 1000 UTC. Vertical wind profile from surface to 700 mb is shown inside the red ellipse.

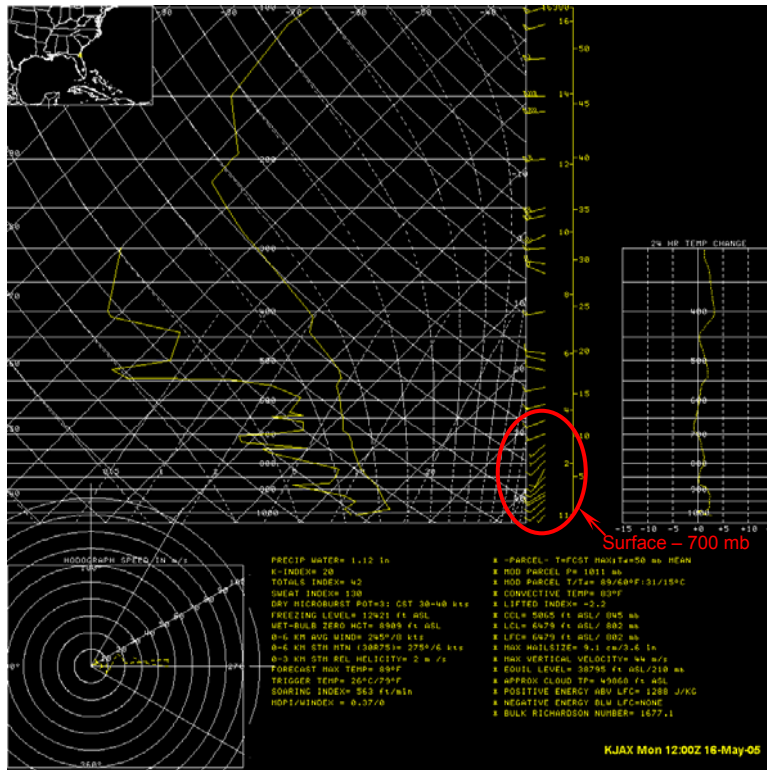


Figure 31. JAX sounding on 16 May 2005 at 1200 UTC. Vertical wind profile from surface to 700 mb is shown inside the red ellipse.

The position of the low-level high pressure ridge and the weak low-level flow played an important role in the development and movement of the cloud bands. In Figure 28, island-generated clouds can be seen extending to the northwest (identified by the yellow circle) from Grand Bahama Island. The low-level wind direction from The Bahamas to the KSC/CCAFS area was southeasterly, which would put these cloud bands on a trajectory towards KSC/CCAFS. However, the cloud bands did not move very far from the island since the winds were so light. Additionally, the low-level winds at the latitude of KSC/CCAFS were more southerly, which would oppose cloud band movement toward the Florida peninsula from KSC/CCAFS northward.

As shown in Figure 28, the east coast sea breeze front was located very close to the east coast in central Florida and curved westward in south Florida due to the prevailing southeasterly flow in that region. Clear skies were evident behind the sea breeze front in the area of subsidence. This was another factor that limited development of cloud bands on this day. Analysis of visible satellite imagery and surface observations indicated that the east coast sea breeze front moved about half way across the state and produced showers and thunderstorms upon colliding with the west coast sea breeze near Orlando, but the east coast remained rain-free with little or no cloud development behind the front.

4.2.2 Analysis of Upper-level Features

A westerly 95 knot jet streak at 250 mb was observed in the Gulf of Mexico southwest of south Florida. Figure 32 shows the position of the Eta 6-hour forecast of the 250 mb jet streak valid 16 May 2005 at 1800 UTC and is overlaid on the visible satellite image at 1745 UTC. The position of the east coast sea breeze front, jet streak right and left entrance regions are identified. East central Florida was on the periphery of the left exit region of the jet streak. The KSC/CCAFS area was probably far enough away from the influence of upper level divergence and therefore the subsidence behind the east coast sea breeze was dominant and suppressed any cloud development.

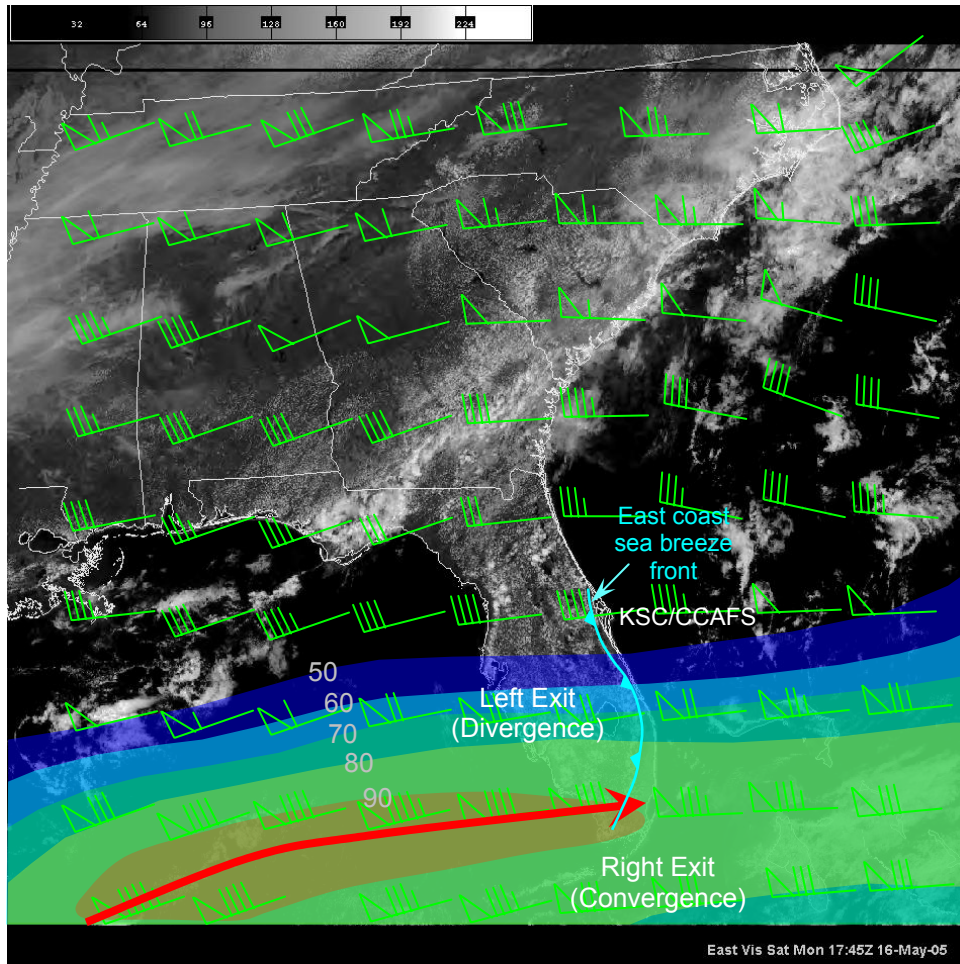


Figure 32. Eta 6-hour 250 mb wind forecast valid 16 May 2005 at 1800 UTC. Wind barbs (knots) are in green. Isotachs are shaded at 50, 60, 70, 80 and 90 knots. The Eta data is superimposed on the visible satellite image on 16 May 2005 at 1745 UTC. The position of the east coast sea breeze front is shown in cyan.

5 Summary and Conclusions

Clouds and precipitation affect a multitude of operations from daily ground processing to space launch and landing. Southeasterly synoptic flow can produce a variety of weather conditions over KSC/CCAFS from clear skies to convective showers and thunderstorms under what appear to be similar synoptic conditions. Because of this, the 45 WS finds that southeasterly flow creates a difficult forecast situation. They requested that the AMU investigate southeasterly flow cases to try and determine the factors that result in different weather conditions and provide forecast guidance on when these convergence bands occur and whether they will produce weather phenomena that will adversely affect operations.

The AMU collected data from April 2005 through February 2006. During the data acquisition portion of this task, the AMU discovered that the convergence cloud band phenomenon not only occurred during southeasterly synoptic flow but during all easterly synoptic flow conditions. Therefore, the AMU collected data from 33 days for this task for days when any synoptic onshore flow occurred. The data collected included visible, infrared and water vapor satellite imagery, upper air soundings, surface observations (including buoy and ship reports), upper air observations, model data (Eta, RUC and ARPS), radar imagery, lightning plots and SST.

Based on a literature review and available data, the AMU evaluated atmospheric stability, low-level wind and pressure patterns, upper-level dynamics, east coast sea breeze position and movement, and SST variations. The data analysis showed indicators which will assist forecasters determine when cloud bands and convective precipitation will move onshore affecting operations.

5.1 Important Forecast Indicators

Several different parameters were analyzed for their capability of forecasting these events, but most did not appear to have any relationship to cloud band development or dissipation. Such parameters included morning sounding stability parameters, temperature or temperature gradients and SST. The combination of certain low- and upper-level phenomena did show some relationship to the formation of these convergence cloud bands.

5.1.1 East-central Florida Low-Level Parameters

The key low-level factors found to be related to convergence band formation in easterly flow are the

- Layer average surface to 700 mb wind speed and direction,
- Location of the low-level high pressure ridge, and
- Location and movement of the east coast sea breeze front.

When the layer-average wind speed was relatively strong (> 8 knots) cloud bands were more likely to cross the coast and move inland. The layer-averaged direction, or cloud-level steering flow, was an important consideration in addition to wind speed. This related to the position of the low-level high pressure ridge relative to KSC/CCAFS. The amount of curvature in the layer averaged streamlines was important in analyzing the trajectory of the cloud bands. Using high resolution (< 12 km grid spacing and < 60 minute forecast periods) model output is a good tool to use for determining these indicators.

The presence or development of the east coast sea breeze front is also important to combine with the layered wind and low-level ridge location analyses. The data from this task indicated if the east coast sea breeze front was developing or was located in the eastern half of peninsular Florida, subsidence behind the front generated in the offshore return flow aloft inhibited the cloud band development and supported cloud band dissipation. Once the sea breeze front had moved west of the center of the state, the subsidence was less of an inhibitor for cloud development.

5.1.2 East-central Florida Upper-Level Parameters

The key upper-level parameters that had an affect on the formation and maintenance of the convergence cloud bands were influences from a jet streak at 250 mb:

- Location of jet streak left entrance and right exit regions and their associated upward motions
- Areas of divergence or convergence.

While jet streaks can be very subtle over Florida, their effects were still found to be important. Figure 21 shows that the divergent regions of a jet resulting in upward motion are in the right entrance and left exit regions. Areas at the surface under these areas could experience enhanced cloud growth. Conversely, the left entrance and right exit regions are areas of convergence and subsidence, and could cause inhibited cloud growth at the surface. No speed or shear thresholds could be determined from this dataset but forecasters should consider any area of upper level divergence or convergence to have an effect on the cloud band development and maintenance.

5.2 Combining the Low- and Upper-Level Indicators

All easterly flow days are not alike and careful analysis of each easterly flow situation based on the criteria described in the section above will help produce a better forecast. Although important in some situations, the influence from the upper-level parameters was not as great as that from the low-level parameters. The results of this task showed that if the convergent area of a jet streak was in the KSC/CCAFS vicinity, it enhanced the subsidence behind an existing east coast sea breeze. However, in the presence of divergence aloft, the dataset used in this task indicated the subsidence behind the sea breeze front had the greater influence on the cloud bands in most of the cases. The relative strength of the upper level divergence based on the position, movement and strength of the jet streak is an important since it may be enough to negate the low level subsidence.

It is important, therefore, to consider the direction and speed of the low-level flow, the existence and location of an east coast sea breeze front, and the areas of upper-level convergence and divergence concurrently when attempting to forecast the existence of convergence cloud bands and any associated weather phenomena that could adversely affect operations.

References

- Augstein, E., H. Riehl, F. Ostapoff, and V. Wagner, 1973: Mass and energy transports in an undisturbed Atlantic trade-wind flow. *Mon. Wea. Rev.*, **101**, 101–111.
- , H. Schmidt, and F. Ostapoff, 1974: The vertical structure of the atmospheric planetary boundary layer in undisturbed trade winds over the Atlantic Ocean. *Bound.-Layer Meteor.*, **6**, 129–150.
- Brümmer, B., E. Augstein, and H. Riehl, 1974: On the low-level wind structure in the Atlantic trade. *Quart. J. Roy. Meteor. Soc.*, **100**, 109–121.
- Chen, Y. and J. Feng, 2001: Numerical Simulations of Airflow and Cloud Distributions over the Windward Side of the Island of Hawaii. Part I: The Effects of Trade Wind Inversion. *Mon. Wea. Rev.*, **129** 1117-1134.
- Uccellini, L. W., and P. J. Kocin, 1987: The interaction of jet streak circulations during heavy snow events along the east coast of the United States. *Wea. Forecasting*, **2**, 289-308.

List of Abbreviations and Acronyms

| Term | Description |
|-------------|---|
| 45 WS | 45th Weather Squadron |
| AMU | Applied Meteorology Unit |
| ARPS | Advanced Regional Prediction System |
| ATEX | Atlantic Trade Wind Experiment |
| AVHRR | Advanced Very High Resolution Radiometer |
| AWIPS | Advanced Weather Interactive Processing System |
| CCAFS | Cape Canaveral Air Force Station |
| ESRL | Earth System Research Laboratory |
| GOES | Geostationary Operational Environmental Satellite |
| GSD | Global Systems Division |
| KSC | Kennedy Space Center |
| JAX | Jacksonville, FL rawinsonde station identifier |
| LWO | Launch Weather Officer |
| MFL | Miami, FL rawinsonde station identifier |
| MYNN | Nassau, Bahamas rawinsonde station identifier |
| NOAA | National Oceanic and Atmospheric Administration |
| NWS MLB | National Weather Service Forecast Office in Melbourne, FL |
| POES | Polar Orbiting Environmental Satellite |
| RUC | Rapid Update Cycle |
| SST | Sea Surface Temperature |
| UTC | Coordinated Universal Time |
| XMR | Cape Canaveral, FL rawinsonde station identifier |

NOTICE

Mention of a copyrighted, trademarked or proprietary product, service, or document does not constitute endorsement thereof by the author, ENSCO Inc., the AMU, the National Aeronautics and Space Administration, or the United States Government. Any such mention is solely for the purpose of fully informing the reader of the resources used to conduct the work reported herein.
